People's Democratic Republic of Algeria
Ministry of Higher Education and Scientific Research
Echahid Hamma Lakhdar University, El-oued
Faculty of science exact
Department of physics

Thesis

Presented to obtain the degree of

DOCTORATE

Specialty: applied physics

Theme

The effects of superstatistics on nonthermal and superthermal distributions on plasma

Presented by: **Fadhila KHALFAOUI**

Puplicly defended: ....

To the jury :

Mr. Elhabib GUEDDA	Professor	University of El-Oued	- President
Ms. Samia DILMI	MCA	University of El-Oued	- Supervisor
Mr. Abdelmalek BOUMALI	Professor	University of Tebessa	- Co-Supervisor
Ms. Nacira BEDIDA	MCA	University of El-Oued	- Examiner
Mr. M. Tayeb MEFTAH	Professor	University of Ouargla	- Examiner
Mr. Said DOUIS	Professor	University of Ouargla	- Examiner

Academic year: 2022/2023

To …

Mom's soul

My grandmom *Dadda*

My father

My brother *Mohammed*

My sister *Sabrina*

Acknowledgments

First and foremost, I would like to praise and thank Allah, the Almighty, who has granted me countless blessings, knowledge, and opportunity to me, so that I have been finally able to accomplish the thesis.

I would like to thank my supervisor – Ms. Samia DILMI –. Support and guidance from you have been invaluable throughout the project.

I would thank Mr. Abdelmalek BOUMALI in particular you've been a fantastic co-supervisor, and who helped me get to this stage.

Many thanks to Mr. Elhabib GUEDDA for accepting to be the president of the committee. I would like to thank the jury members Ms. Nacira BEDIDA, Mr. Mohammed Tayeb MEFTAH, and Mr. Said DOUIS.

My gratitude extends to the Science Exact Faculty at El-Oued University. Additionally, I would like to express gratitude to Ms. Souhaila ASKRI, whom I learned so much. I would like to thank the configuration team for the cherished time spent together.

My appreciation also goes out to my family "grandmom, my father, Mohammed, Sabrina, and my aunty Badiaa" for their encouragement and support all throughout my studies, thank you all for your support and input.

Contents

List of Figures

Notation

ΔE	energy amount
α	ionization degrees
$(j, N_j), (k, N_k)$	the population of ions state
E	energy, electric field
B	magnatic field
k	species of particles
n, l, m	principal quantum number
n_e	electron's concentration
Z	atomic number, normalization constant
g_i, ω	statistical weight
T	temperature
k_B	Boltzrnann's constant
h	Planck's constant
b	constant
c	speed of light
v	velocity, frequency
ρ	photon distribution
A, X	transition or ionization rates
S	electron spin
J	total angular momentum
a_0	radius of the first Bohr orbit of atomic hydrogen
hv	photon energy
E_B	binding energy
k_0	kinetic momentum
E_k	kinetic energy
σ	cross section
R_y	Rydberg constant
n, i, j	statistical state
a	DR rate coefficients
N	electron target state
A^r	radiative A rates
P_{rad}	radiated power
$\overline{\phi}$	energy
I	ionization energy
q_0	reasonable estimation
I	ionisation potential
A, B_i	Dtting coefficients
Q_k	identical to that for EIE
Ω_{01}	collision strength

g_0	statistical weight of the initial state
κ	relativistic angular quantum number
m	mass of electron
ξ_{nl}	number of electrons
U	reduced impact energy
P_i	binding energy
P_1	ionization potential
q_i	number of equivalent electrons
a_i, b_i, c_i	individual constants
A_j, B_j, C_j, D_j	constants
T_N	total number of computed trajectories
b_max	impact parameters below
$b_j^{(c)}$	trajectory's actual impact parameter
f	distribution function
f_{hot}	normalized hot electron fraction
f_M	Maxwell energy distribution function
T_{bluk}	bulk electron temperature
T_{hot}	hot electron temperature
x	independent variable
σ	variance
η	mathematical expectation
(x_{min}, x_{max})	border
μ	Gaussian distribution parameters
$B(E)$	effective Boltzmann factor
β	approximately constant
β_0	average of β
$f(\beta)$	probability density
χ^2	Gamma distribution
Γ	Tsallis statistics function
n	freedom's degree
q	entropic index
EII	Electron Impact Ionization
TE	Thermodynamic Equilibrium
PLTE	Partical Local Thermodynamic Equilibrium
LTE	Local Thermodynamic Equilibrium
CE	Coronal Equilibrium
CRE	Collisional Radiative Equilibrium
EIMI	Electron-Impact Multiple-ionization
DR	Dielectronic Recombination
TBR	Three-Body Recombination
DM	Deutsch-Maärk Cross Section
FAC	Flexible Atomic Code
DW	Distorted-Wave
EIE	electron impact excitation
He	neutral Helium
Be^{+2}	Beryllium like Helium
Li^+	Lithium like Helium

General introduction

Electron-impact ionization (EII) is important in dynamic systems, where it happens when the ions gain suddenly temperatures higher than electrons. For this reason, EII is basic to study solar flares, nanoflare coronal heating, supernova remnants, and merging galaxy clusters. In another hand, EII can also have a super effect on the charge state and non-thermal electron energy distribution for plasmas. For such plasmas, there is a substantial population of electrons in the high energy tail of the distribution that lies above the EII threshold. Thus, EII is relevant to the modeling of astrophysical systems where such non-thermal distributions are present [1].

The plasma represents of 99.9 % of the known cosmos. Ionized matter either exists in the interstellar medium, stars, and more exotic compact objects or surrounds them all. Therefore, one must work hard on plasmas to know the secrets of the universe [2]. Generally, electrons, ions, and neutral particles are the main compounds of plasmas. The most effective approach to creating ions is by ionizing neutral atomic systems via electron impact, by this method results in a significantly greater ratio between ionization cross-section and collision energy than either photon or ion impact [3].

Comparing atomic processes by different codes and simulation methods is an interesting issue in plasmas, which can help to validate the underlying models. In order to use them for diagnostics exacted models have to be reliable. However, checking the reliability of a model requires its comparison with experimental data. This does not exclude model-model comparisons. Therefore, the comparison of the code becomes harder when they include a confrontation with experimental measurements. Also, to a better understanding of various approaches ought to lead to different best plasma parameters.

Besides, electron impact ionization cross sections are important components in the modeling of hot plasmas, both laboratory and astrophysical. The diffi-

culty involved in measuring or calculating electron ionization rates for highly ionized atoms has resulted in the use of a variety of semiclassical and semiempirical approximations based on the limited available data for neutral or charged systems [4]. The last one is dependent on it to calculate the ionization rates, which are known as the quantity of electron-hole pairs produced by a carrier per unit distance [5].

Moreover, The statistics of all observed particles are usually covered by the most two known realizations of quantum statistics: the Bose-Einstein (BE) statistics, and the Fermi-Dirac (FD) statistics. Many complex systems exhibiting fluctuations can be described by decomposing their dynamics at different scales. Their statistical properties are then given by a mixture of statistics, i.e., superstatistics.

Classical particle systems are characterized by the absence of correlations among the individual particle energies. The statistical behavior of these systems has been successfully described by Boltzmann–Gibbs statistical mechanics (BG) and Maxwellian distribution of velocities. Space plasmas are noncollision and correlated particle systems, characterized by stationary states out of thermal equilibrium that exhibits a non-Maxwellian behavior, which is typically described by Kappa distributions [6].

Superstatistics is a branch of statistical mechanics or statistical physics devoted to the study of non-linear and non-equilibrium systems. It is one of the most important and attractive topics in statistic mechanics. Its name is chosen because the new statistics represent a kind of 'statistics of statistics' [7]. And it has become a topic of great interest in the last few years, and it has been finding applications in several branches of physics [8, 9].

On the other hand, the recent works on superstatistics were newer and newer such as Hassanabadi et al. used it on momentum operator with the Dunkl derivative in quantum mechanics and derive its Schrödinger equation in one dimension with a harmonic oscillator potential [10]. And it applied on black hole quasinormal modes [11], analyze the capacity of the superstatistics construction to provide modeling of the velocity field probability density functions of isotropic turbulence [12]. Memristor Current–Voltage Modelling [13]. Additionally, the procedure for obtaining the superstatistical density of states, where the probability density function has the nonzero variance, is first devel-

oped [14].

The aim of this project presents the calculation of ionization rates using the formalism of superstatistics in various ways. We shall introduce the influence of electron energy distribution functions on the calculation of ionization rates for neutral Helium and establish the effects of hot electron fraction. Then, we shall show the influence of superstatistics on non-thermal and superathermal distributions on the calculation of ionization rates for Beryllium, and Lithium like Helium (Be^{+2}, Li^{+}), where we shall replace the distribution function with an effective Boltzmann factor. Finally, we shall discuss the results and present comparisons with old studies that present the influence of electron energy distribution functions on the calculation of ionization rates.

The work developed in this paper according to the following outline:

Chapter 1 deals with a general introduction to plasma. Additionally, It has a background in equilibrium models, which are interesting in statistical physics, and this chapter tells too about various elementary processes in hot plasmas.

Then, *chapter* 2 focuses on theoretical aspects, especially those that appear through atomic collisions. It mentions cross sections, which calculate by several codes in either empirical or semi - empirical ways. Moreover, it presents commonly known distribution functions that are basic in quantum mechanical systems. Also, it shows superstatistics distribution with the ionization rates coefficients of atoms and ions.

While *chapter* 3 shows the calculation of the ionization rates of neutral Helium, Beryllium, and Lithium like Helium using the superstatistics concept, then they are compared with another experimental result.

Finally, this work finishes with a *general conclusion*, which summarizes the highlighted results of various calculations.

References

[1] S. Dilmi, A. M. Boumali, U.P.B. Sci. Bull. Series A, Iss. 1, 79, 249–260, (2017).

[2] R. P. Drake, High Energy Density Physics, Springer, Library of Congress Control, Netherlands, (2006).

[3] T. D. Mark, plasma physics and controlled fusion, vol. 32, No. 13, 2083-2090, (1992).

[4] S. M. Younger, Quant Spectrosc Radial Trans, vol. 27, No. 5, 541-544, (1982).

[5] W. Maes, K. Meyer, R. V. Overstraeten, Solid-State Electronics, vol. 33, No. 6, 705-718, (1990).

[6] G. Livadiotis, Kappa Distribution: Theory & Applications in Plasmas, 1st Ed, Elsevier: Amsterdam, The Netherlands; London, UK; Atlanta, GA, USA, (2017).

[7] C. Beck, E.G.D. Cohen, Physica A, 322, 267–275, (2003).

[8] A. Boumali, F. Serdouk, S. Dilmi, Physica A, 124207, (2020).

[9] F. Khalfaoui, S. Dilmi, A. Boumali, Physica A, 596, 127193, (2022).

[10] H. Hassanabadi, M. Montigny, W. S. Chung, P. Sedaghatnia, Physica A, vol. 580, 126154, (2021).

[11] A. M. Merino, M. Sabido, Phys. Lett. B, vol. 829, 137085, (2022).

[12] E. Gravanis, E. Akylasa, C. Michailides, G. Livadiotis, Physica A, vol. No.567, 125-694, (2021).

[13] R. Konlechner, A. Allagui, V. N. Antonov, D. Yudin, SSRN Electronic Journal, (2022).

[14] W. S. Chung, A. Algin, The European Physical Journal Plus, vol. 137, No. 620 (2022).

Chapter 1

Atomic Processes in hot plasma

1.1 Introduction

In recent years, plasma has had an increasing interest in scientific research; because of its widespread use in wide technology domains such as semiconductor devices [1], compact astrophysical objects, etc.[2, 3]. Actually, plasma is usually described as the fourth state of matter [4], and It is following known phases of a solid, liquid, and gas, the transition from one state to another is put by enough energy amount (ΔE) [5].

$$Solid \overset{\Delta E}{\rightarrow} Liquid \overset{\Delta E}{\rightarrow} Gas \overset{\Delta E}{\rightarrow} Plasma$$

This refers to the four pre-Socratic Greek philosophical elements of Earth (solid), water (liquid), air (gas), and fire. The concept of plasma dates back to "Michael Faraday" (1791–1867), who proposed a radiant state of matter in 1809, which he related to the phenomena that is generated by electric currents flowing in gases [6].

In 1928, an American scientist named "Langmuir" defined plasma as an advanced gaseous state that has positive and negative particles, ions, and electrons, and also neutral atoms and molecules, where the thermodynamic laws are not applied [7]. Despite the fact that plasma science was only called in this year, it is a long-standing branch of physics. Furthermore, the history of electricity is inextricably linked to the origins of plasma physics [6].

Plasma is a basically neutral mixture of electrons and ions; or we can say that it is an ionized gas [8, 9]. In other words, plasma is commonly a system that has many bodies, that are composed of a wide number of charged particles which are dominated by collective effect by the electromagnetic force [10]. Additionally, the motion of single particles is decided by electric and magnetic

forces, which are either external or from their own charge, which determines the plasma's behavior [11]. Because plasma is considered as an ionized gas, and so it has ionization degrees ranging from $0 < \alpha \leq 1$[12].

There is interference in the plasma phenomena and this makes it difficult to study the plasma behavior. Therefore, there are a lot of parameters that determine the exact behavior. One of them is observed during a collision when the particles of gas interact for very short periods; but in the remaining time, each particle has free movement. Moreover, there isn't any interaction when the distances are greater than the size of the gas molecules. This state is explained by the potential energy that is too lower than kinetic energy. Moreover, the ratio of the distance at which particles contact is important if the average distance between particles isn't large [13].

As a result, plasma can be described by Debye length, which depends on the right number of electrons and ions. Also, it should be attentive to the individual contributions of electrons and charged particles[14]. In addition, the degree of ionization determines approximately on too easy grounds. It can find that the ionization energy relates to the temperature of electrons and the relative populations of the ionization states are presented by the Saha equation, which shows the ratio of the population of ions in state (j, N_j), to state (k, N_k) [15]. Saha equation describes the quantity of ionization to be expected in thermal equilibrium conditions, which binds temperature to ion density [16].

On the other hand, the existence of plasma in the universe, leads scientists to classify plasma to simplify its study. Plasma is sectioned into cold (non-thermal), and hot (thermal) plasma on the basis of: the temperature of electrons ionization, atmospheric pressure, and temperature conditions determine these classifications [17]. Firstly, Cold plasmas are generated when the electrons' temperature is higher than the heavy charged particles, and the translational energy of weighty particles stays so low [18].

Additionally; they don't show any thermodynamical equilibrium, at the same time it's an intensive plasma [19]. Secondly, hot plasmas are a completely ionized medium and distinguish by a long mean free path with kinetic pressure [20], and they are in thermal equilibrium with each other [21] when the temperature of the electron and the ion is the same [22].

In fact, plasma science becomes an advantage to future technology, given that we can see the fourth state of matter everywhere. Sun produces the thermal radiation that makes the Earth habitable, which is the most important plasma object in our universe. It is a functional steady-state fusion reactor that turns protons into heavier elements and beams energy [23].

In 1908, physicist Kristian Birkeland named the flow of charged particles from the Sun the solar wind [24]. There are two sorts of plasma flows, the slow solar wind that is created in the coronal streamer belt at low heliospheric latitudes, and the fast solar wind from coronal holes at high heliospheric latitudes [6]. Besides, one of the traditional sectors for plasma applications is lighting. For street lights, electric arcs in high-pressure lamps are employed, whereas low-pressure discharges in fluorescent tubes are used for office and household lighting [25].

The passing of electron beams through a gas is a frequently used technique for producing plasma. Then, specific processes can take advantage of secondary electrons such as secondary electrons in exciter lasers which are accelerated by an external electric field to produce excited molecules with brief lifetimes because the ionization process lasts only a short time, using an electron beam as a source of ionization [26].

Flames are used as a chemical technique for producing plasma. The reagents have chemical energy to create radicals or excited particles, and the process is called chemoionization which includes charged particles. Therefore the amount of ionization in flames is little because the conversion of chemical energy into the energy of ionized particles is inefficient [26].

1.2 Plasma equilibrium models

1.2.1 Thermodynamic Equilibrium (TE)

Thermodynamics deals the heat and its ability to generate motion. Over time, it evolved into a theory that defines state of matter transformations, with heat generated motion being a result of specific transformations [27].

In addition, the thermodynamic equilibrium comprises a thermal and mechanical equilibrium, as well as the internal equilibrium which occurs when there is no heat flow in a system, resulting in the same temperature in all areas

of the system whereas the mechanical equilibrium implies no external forces and no pressure gradient inside the system [28].

Besides that, Maxwell, Boltzmann, Saha, and Planck are the four mechanisms of balance in a system under thermodynamic equilibrium. So, TE needs all microscopic processes balanced statistically by the inverse process [29].

The Planck law depends on a radiation equilibrium, while the Maxwell distribution relates to the kinetic energy of particles of species k, the Boltzmann distribution for the density of excited atoms, and the Saha distribution studies the density of excited neutral atoms with respect to the density of the ion ground level, which sets the degree of ionization. All of the temperatures are equivalent in TE and correspond to the thermodynamic temperature [29].

Now, we show the four types of balances in a system under thermodynamic equilibrium:

★ Planck's balances

$$A_q \longleftrightarrow A_p + h\upsilon \tag{1.1}$$

absorption $\longleftrightarrow$ spontaneous emission $\rightarrow$ stimulated emission

★ Maxwell's balances

$$\begin{gathered} X + Y \longleftrightarrow X + Y \\ E_X + E_Y = (E_X + \Delta E) + (E_Y - \Delta E) \end{gathered} \tag{1.2}$$

Kinetic energy exchange and conservation

★ Boltzmann's balances

$$X + A_p + E_{qp} \longleftrightarrow X + A_q \tag{1.3}$$

deexcitation $\longleftrightarrow$ excitation

★ Saha's balances

$$X + A_p + E_{ip} \longleftrightarrow X + A_1^+ + e \tag{1.4}$$

$recombination \longleftrightarrow ionization$

Conversely, The degree of interaction between the compounds in laboratory plasma is insufficient to create a comprehensive balance on all processes necessary for TE [30]. Furthermore, when a small quantity of the produced radiation is not reabsorbed in the plasma, the weakest form of TE departure occurs, and also Planck's law isn't obeyed in this way. On the other hand, the equilibrium condition of the Maxwell, Boltzmann, and Saha balances can be maintained if the photon energy outflow is less than the energy of the collision, while the ions, atoms, and electrons stay at the same temperature. Because of the possibility of multiple spatial gradients, local thermodynamic equilibrium is the most appropriate one at this state [30].

1.2.2 Particle Local Thermodynamic Equilibrium (PLTE)

The electron density is substantial to get full local thermodynamic equilibriums that are not extremely high. They trigger overpopulation that at the fundamental level and hence radiation transitions are substantial. Consequently, the electron density for PLTE is written as [31]:

$$n_e \geq 7.10^{18} \frac{Z^6}{n^{\frac{17}{2}}} \left(\frac{T}{E_{iz}} \right) \tag{1.5}$$

Where n is the principal quantum number of the lowest level in the PLTE, E_{iz} is the ionization energy, Z is the atomic number, n_e is the electron's concentration.

1.2.3 Local Thermodynamic Equilibrium (LTE)

At the macroscopic level, the idea of local thermodynamic equilibrium is fundamental to nonequilibrium thermodynamics, and it appears in certain statistical mechanical models, such as the quantal and the classical models[32].

In the discipline of plasma spectroscopy, LTE is very essential. In this case, the plasma state at a position (r) at the time (t) is calculated if, for example, the parameters of total pressure and local temperature are known. As a rule, all thermodynamic laws for thermodynamic equilibrium also apply in local thermodynamic equilibrium, but there is an exception with Planck's radiation law [33].

Moreover, LTE is utilized frequently to ease the interpretation of spectral line intensities in either the laboratory or astrophysical plasma. As a result,

spectroscopic methods for determining electron temperature T and density n, have been developed. It's also useful in experimental atomic physics, such as determining the probability of an atomic transition from a line intensity observation. As a result, in order to conduct a good analysis, it is necessary to have very exact criteria to determine the plasma parameters under which it is acceptable to presume LTE [34].

Local thermodynamic equilibrium is described by the population density (n_i) of quantum level on the basis of the collisional-radiative model, the populations are mightily impacted by thermal collisions between plasma species when the radiative rates are less than collisional rates as well as the equivalent Saha density (n_i^{Saha}), it is calculated as [33, 35]:

$$\frac{n_e n_{z,1}}{n_{z-1,i}^{Saha}} = \frac{2g_{z,1}}{g_{z-1,i}} \frac{(2\pi m_e T)^{\frac{3}{2}}}{h^3} exp\left(-\frac{E_{z-1,z}^{(i)} - \Delta E_{z-1,z}}{k_B T}\right) \tag{1.6}$$

Where g_i is the statistical weight, T is electron temperature, k_B is Boltzrnann's constant, h is Planck's constant, $(E_{z-1,z}^{(i)} - \Delta E_{z-1,z})$ is the ionization potential.

The spectroscopy allows determination of the electron density and temperature by means of the eq.(1.6), when b_i equals unity within 10 % or better, a level is considered to be in partial LTE in following equation [33]:

$$n_i = b_i n_i^{Saha} \tag{1.7}$$

The higher levels of ions run to a thermal distribution with the continuum of free electrons facilely than the downer levels, which accords to collisional radiative process theory. As a result, the concept of LTE is valid [34].

The photon distribution is given by a Planckian (thermal) radiation field at temperature $k_B T$ [36].

$$\rho(\upsilon) = \frac{2h\upsilon^3}{c^2} \frac{1}{e^{\frac{h\upsilon}{T}} - 1} \tag{1.8}$$

Where, c is the speed of light, and υ is the frequency.

However, if the equilibrium is just local, photons will not obey the Planck law. This happens because photons can quickly escape from a specific zone

of the plasma. The optically thin plasma is the subject of this case. The presence of temperature and density gradients causes the difference between an equilibrium [36].

1.2.4 Coronal Equilibrium (CE)

Coronal equilibrium is obtained at the lowest densities in optically thin plasmas, where the collisional excitation rate is down in contrast to spontaneous decay. Consequently, the population of the ground state is quite large in comparison to the population of the excited levels. When the electron density is close to zero, the populations of ground and excited levels tend to be 1 and 0 respectively. Furthermore, there is a weak chance of finding two free electrons nearby the ion at low density, so the recombination process has a minimum rate, and the dominant processes that govern average ionization are electron impact ionization and autoionization, radiative recombination, and electron capture. Since the contribution of the autoionization process is independent of temperature and density, whilst the contribution of electron impact ionization decreases as density increases, autoionization is a very important ionization mechanism in the CE regime [37].

For example, in a Hydrogen system that has atomic number Z, collisional recombination is dominated by radiative recombination [38], so:

$$n_e \leq 5,9.10^{10} Z^6 \sqrt{T_e} exp\left(\frac{0,1Z^2}{T_e}\right) \tag{1.9}$$

1.2.5 Collisional Radiative Equilibrium (CRE)

All the previous initial transmissions describe the plasma populations, where the temporal evolution of the population of each ion's level is governed by the processes of population and depopulation to other levels:

$$\frac{dN_{Z,i}}{dt} = \left(\sum_{Z'j \neq i} \tau_{Z'j,Z'i} N_{Z'j}\right) - \left(\sum_{Z'j \neq i} \tau_{Zi,Z'j}\right) N_{Z,i} \tag{1.10}$$

Where the $\tau_{Z'j,Z'i}$ are the transition rates from level j of ion Z' to level i of ion Z.

The populations and depopulations for each atomic state (i) are balanced if a stable state exists $\frac{dN_{Z,i}}{dt} = 0$, when the temperature and the density evolution

are slow, the plasma is called quasi-stationary, and the excited population levels equilibrate quasi-instantaneously to ground states, which are described in an unstable [39].

1.2.6 Photoionization Equilibrium

Photoionization is an ionization process to plasma that too low densities, and the radiative field is very intense in which the process is equilibrium by radiative recombination (τ^{rr}), as follows [40]:

$$\frac{n_{Z+1}}{n_Z} = \frac{\tau^{photo}_{Z,Z+1}}{\tau^{rr}_{Z+1,Z}} \tag{1.11}$$

1.3 Elementary processes in plasmas

1.3.1 Ionization

Any element's atomic structure contains a positive nucleus, which has the biggest mass surrounded by one or more electrons in orbital motion. Besides, the binding force of electronic energy, which is usually controlled by the ionization and also the pulsing and gyrating motion of an electron, requires enough amount of energy to hold their paths in various shells. The interactions between electrostatic repulsion and interactions with their magnetic moments are highly complex for the atoms that have multi-electron, and they influence the ionization process. In the case of a partially full inner shell, the Pauli principle must be followed to the total of the shell. As well, the chemical activity of the atom is influenced by whether the electron shells are fully or partially filled [41].

Both atomic and molecular ionization processes are identical, even if molecular processes have some complications due to the rise inner degrees of freedom. Generally, many ways share in production energy by highly excited states of atoms and molecules such as thermal, chemical, electrical, and radiative resources. During the collision process, the ionizing mechanism is the most commonly used. The depletion process involves dissociation, dielectric recombination, and electron attachment, while the inelastic collision process involves inelastic collision, electron impact, radiative interactions, and charge exchange [42].

In the laboratory, plasma is generated basically by electron impact ionization, where energy is supplied by an external electric field and it is transferred through elastic and inelastic collisions. The characteristic ionization temperature is always higher than the partially ionized gas temperature, and the ionized components rarely achieve thermodynamic equilibrium. At the outer limits of the Maxwellian distribution, high-energy electron collisions ionize atoms; electron avalanches formed in an electric field evolve in time and space along the drift direction of free electrons. As a result, the ionization frequency is not used to determine the rate of electron impact ionization but used the ionization coefficient ($\alpha = \nu/u_d$), which is proportional to the particle collision frequency α and the electron drift velocity u_d. The secondary emission, which produces breakdown for discharge within the electrode gap is sustained by a little amount of electric current [43].

Evidently, when a valence electron collides with an incident electron and gets more energy than the atomic ionization potential, ionization occurs. The Townsend Similarity law describes the ionization [44].

Ionization is the process of releasing electrons from the bonds that hold atoms together. The process of ionization is oftentimes linked to the process of deionization. The influence of ionization processes is based on the gas pressure, which is a variable that indicates the random thermal energy of particle movement. Particles per unit volume and energy per particle combine to form pressure. Higher energy per particle gases at low pressure ionize more readily[45].

The atomic model is too important to determine crucial ionization in the quantum, electrons set in orbits that have various energies. It is simpler to ionize electrons in the external shells because they are bonded to the nucleus with lower energies. An electron must receive energy during the ionization process that is larger than the energy holding it in its atomic shell. Collisions between electrons, ions, neutral atoms or molecules, radiation, and other particles can all provide this energy [45].

On the other hand, atomic ionization via another electron impact mechanism for plasma formation is also a possibility. An atom can be ionized through a series of excited states after being initially stimulated by collision, raised to a higher energy state, then ionized. The procedure in this instance is known as

stepwise ionization, the one-step ionization is also regarded as direct ionization [41].

1.3.2 Excitation

Excitation is an electron's transmission from inner orbits of an atom or molecule to an outer orbit, commonly through collision with a free electron. Normally it is the outer orbit since this requires the least energy. The process of electronic excitation of an atom is given by [46]:

$$\begin{cases} e + A & \rightarrow A^* + e \\ A^* & \rightarrow A + hf \end{cases} \tag{1.12}$$

This phenomenon is accompanied by the emission of energy often as light at a wavelength uniform to the excitation energy.

When electrons of plasma collide with an ion that has charge Z, the last can go into an excited state, or de-excite by absorbing the energy of the incident electron. These processes result in balance [47].

Electronic excitation is among the essential concepts in chemistry, physics, and materials science since it has significance in optical absorptions, reflections, emissions, magnetism, and other phenomena. The term "quasi-particle", or "exciton", which is defined as a pair of excited electrons and holes is bound by Coulomb interaction originating in their mutually opposed charges, is used to characterize these events. This idea is used to interpret optical absorption, emission, and spatial excitation propagation [48].

The optical excitation techniques and the electrical ones are very similar. With electrons, the selection criteria are far less strict, allowing for the populating of a far greater number of atomic and molecular levels. Both pulsed and sinusoidally modulated excitation can be employed, just like in photon studies [49].

The evolution of lasers has made it possible to advance the optical excitation of atoms and molecules very quickly, and a pulsed nitrogen laser is usually utilized. In contrast, numerous levels can be occupied at once during electron excitation, which is typically less selective than photon excitation [49].

1.3.3 Transitions radiatives

A radiative transition is one in which the energy is an emission such as a photon. This emission is determined by the initial and final state's properties as well as the pathway of the excited state. A set of standards for electric dipole transitions governs the permitted radiative transitions between atomic energy levels. Firstly, there are no restrictions on the quantum number n. Moreover, resonance transitions which can theoretically be seen in both absorption and emission, are transitions between the ground and an excited atomic level [50].

On other standers, if the quantum numbers l, m modify by the amounts of the radiative transitions between the states nlm, $n^{'}l^{'}m^{'}$ possible.

$$\begin{aligned} \Delta l &= l^{'} - l = \pm 1 \\ \Delta m &= m^{'} - m = 0, \pm 1 \end{aligned} \tag{1.13}$$

The dipole radiation selection rules are known at eq. (1.13), which refers to allowed transitions. Besides, dipole radiation is blocked when eq. (1.13) is not done [51].

Electric dipole transitions can only bind levels of the opposite valence because the electric dipole moment operator is extra special to with respect the inversion of the coordinates. In another case, the electric dipole moment operator does not include the electron spin account, therefore it must have $S = 0$. Concerning heavy atoms, where the spin-orbit splitting is very great, this law is not used. The stringent selection rule for the total angular momentum J is $J = 0, 1$, however transitions from $J = 0$ to $J = 0$ are not permitted [50].

1.3.4 Photoionization

One of the most interesting interactions between radiation and matter is the photoionization of atoms, which is significant in various scientific domains. The photoionization from excited states has numerous applications, such as determining crosssections precisely from excited states of atoms. Since the electrons in each of the elements are listed in the Periodic Table and inhabit distinct shells according to their electronic configurations, the ground state atoms can be promoted to excited states by the photoabsorption process. The process of photoionization, in which atoms break down into free electrons and ions, occurs when the outermost bound electron may be disengaged in the presence of high energy radiation [52].

$$Atom + h\nu \longrightarrow ion + e^{-} \tag{1.14}$$

There are a lot of main mechanisms and primary processes in photoionization, which are direct ionization into the continuum, with or not ion excitation, direct dissociative ionization, and direct multiple ionization. Fluorescence from the excited states of the ions, subsequent dissociation from an otherwise stable state of the ion (predissociation), and multiple ionization by Auger events are examples of secondary processes [53].

Through interaction with the electromagnetic field of the incident photon, direct photoionization denotes that an electron is excited out into the continuum. For photon energies are over the threshold energy, it takes a constant amount of energy, therefore the difference of energy between the ground and ionized states to remove an electron from the molecule or atom and out into the continuum. Common names for this constant quantity of photon energy include threshold energy, ionization, and binding energy (E_B). The binding energy is independent of photon energy far above the threshold, and due to the need for energy conservation, the kinetic energy of the photoelectron (E_k) is determined by the difference between photon energy and the binding energy [54]

$$E_k = h\nu - E_B \tag{1.15}$$

Eq. 1.15 indicates that the binding energy of a specific electronic level can be determined by observing the kinetic energy distribution of the photoelectrons of the energy of the incident photons. Molecular orbitals are separated into valence and core orbitals. The beginning is when valence orbitals diffuse orbitals that are building the molecular bond, and core orbitals, which are primarily associated with a particular atom and do not take place in the molecular bonding. A valence level's binding energy is often orders of magnitude lower than a core level's binding energy [54].

1.3.5 Recombination

Recombination can be a too hard process because most plasmas contain various ion species and charges. The normal outcome of ion-ion recombination is an excited electron, which is followed by radiation emission [45].

Recombination of electron-ion is an exothermic process in which a free electron is caught by an ion after the collision. with moderate and low electron densities [55].

Moreover, ion plasma recombination processes differ from electronic plasma recombination in a few specific ways, where the neutral number density is higher than the ion number density in ion plasma. As a result, there are much more collisions between ions and their neutral counterparts than between ions themselves. Besides, the comparatively low temperature of ions and neutrals allow the creation of complex cluster ions. When compared to electron-ion plasmas, the effect of the aforementioned components can be liberated of the recombination rate caused of the Coulomb nonideality [56].

The presence of a third particle or an environment to absorb the extra energy is required for the recombination of an electron and an ion, whereas the condition is sufficient for the recombination of two ions when the distance between them shrinks enough to allow a tunneling transfer of an electron from the negative to the positive ion [56].

There are three recombination types that are called radiative recombination, dielectronic recombination, and Three-body recombination.

◇ Radiative Recombination (RR)

Radiative recombination is a non-resonant mechanism in low-density plasma, where a free electron recombines an ion and liberates extra energy as a photon [55, 57].

$$X^{q+} + e^{6} \longrightarrow X^{q-1} + h\nu \tag{1.16}$$

Considering, $h\nu$ is the photon energy

$$h\nu = E_e + E_b \tag{1.17}$$

Where E_e is the free electron's kinetic energy and E_b is the state's binding energy when the free electron is captured.

Radiative recombination can be possible at any collision energy, and there is a finite probability that the ion will recombine into any of its obtainable levels. Kramers theoretically deduced the first equation for the RR cross sections for bare ions interacting with free electrons in 1923, using the semi-classical approach [55].

$$\sigma_{RR} = 2,105.10^{22} \frac{R_y^2 Z^4}{nE_e\left(n^2 E_e + R_y Z^2\right)} \tag{1.18}$$

R_y is the Rydberg constant, while n is the ion's primary quantum number.

Also, accurate cross sections for electron capture into high n states are provided by eq.(1.18).

◇ Dielectronic Recombination (DR)

Dielectronic recombination is a successful mechanism in high temperatures. This mechanism for the creation of ionization equilibrium in the solar corona. Because of it, spectral lines that are satellites to the resonance lines of the highly ionized systems typical of hot plasmas can be seen on their long-wavelength side. These lines can also be created for the heavier ions by directly exciting an inner shell electron [58].

Massey and Bates (1942) were the first to identify the dielectronic recombination process in which a recombining ion captures a free electron without emitting radiation, and so creating a doubly excited quasi-bound state, which is then followed by the emission of radiation, creating a stable singly excited state in the recombined ion. The ionization equilibrium and time history of the generating plasma may be significantly impacted, and it is more effective than the typical radiative recombination process [58].

During dielectronic recombinationDR, a free electron collisionally stimulates an ion while also it is captured into the recombined system's autoionizing state. If the ensuing doubly-excited state goes on to radiatively decay below the initial ionization threshold, DR has taken place. Over a wide variety of electron temperatures, densities, plasma timeframes, level populations, and the ionization balance of plasmas must be calculated using DR rate coefficients. The DR rate coefficient from an initial metastable state v to a final state i is given a [59].

$$\sigma_{DR} = \left(\frac{4\pi\alpha_0^2 I_H}{T_e}\right)^{\frac{3}{2}} \sum_j \frac{\omega_j}{2\omega_v} e^{\frac{E_c}{T_e}} \frac{\sum_l A^a_{j\to v,E_c l} A^r_{j\to v}}{\sum_h A^r_{j\to h} + \sum_{m,l} A^a_{j\to m,E_c l}} \tag{1.19}$$

Where ω_j is the statistical weight of the $(N+1)$ electron doubly-excited resonance state j, ω_v is the statistical weight of the N electron target state and

the autoionization A^a and radiative A^r rates are in inverse seconds, E_c is the energy of the continuum electron of angular momentum l.

I_H is the ionization potential energy of the hydrogen atom, k_B is the Boltzmann constant, T_e is the electron temperature and $(4\pi\alpha_0^2)^{\frac{3}{2}} = 6,6011.10^{-24} cm^3$

◇ Three-Body Recombination (TBR)

Three-body recombination is important for various applications to plasma modeling. In a TBR, one electron and an ion combine together while the other electron absorbs the extra energy to depart. The research dates back to the 1960s when traditional techniques were used. In classical techniques, the three-body recombination has two main predictions, the first is the rate of TBR scales as $\sim T^{-\frac{9}{2}}$, and the second, it would likely fill the energy level n_0 so that the binding energy $|E_n| \sim k_B T$, where T is the electron temperature in plasma. The latter was too referred to as the "bottleneck" theory [60].

Despite that three-body recombination has been experimentally investigated and proven to be less prevalent in high-temperature plasmas, it may be essential for the electron's energy lowers [61].

Three particles collide in the process creating a two-body bound state and a free atom. When two objects collide, the binding energy which is typically much greater than the depth of the trap is then released as kinetic energy, causing inelastic losses [60].

1.4 Conclusion

In this chapter, we have provided some background introduction to plasma, and then different plasma equilibrium models were presented. Elementary processes in hot plasmas have been also discussed.

References

[1] R. M. Abolfath, A.G. Petukhov, I. Zutic, Phys. Rev. Lett. 101, 207202 (2008).

[2] L. Silva, O. R. Bingham, J. M. Dawson, J. T. Mendonca, P. K. Shukla, Phys. Rev. Lett. 83, 14 (1999).

[3] A. Atteya, E. E. Behery,W.F. El-Taibany, Eur. Phys. J. Plus, 132: 109, (2017).

[4] T. Makabe, Z. Petrovic, plasma electronics: application in microelectronic device fabrication, CRS press Taylar&Francis group, LLC Boca Raton, US, p1, (2006).

[5] J. L. Raimbaul, introduction à la physique des plasmas, université Pari-Sud11, master 2APIM et PIE, (2013).

[6] A. Piel, Plasma Physics: an introduction to laboratory, space, and fusion plasmas, Second Edition, Springer Nature, Springer International Publishing AG, Switzerland, (2017).

[7] J. Ruzbarsky, A. Panda, Plasma and Thermal Spraying, Springer Briefs in Applied Sciences and Technology, Springer Nature, Switzerland, (2017).

[8] Y. Elskens, D. Exend, microscopic dynamicsne of plasmas and choas, Institue of physics publishing, whollyowned, London, British, (2003).

[9] U. S. Patent, beat frequency modulation for plasma generation, US, 6309, 978B1, (2001).

[10] F. Haas, quantum plasma a hydrodynamic approach, Springer series on atomic. Optical and plasma physics 65, science business. Media. LLC, (2011).

[11] G. J. Pert, foundations of plasma physics for physicists and mathematicians, 1st ed, Wiley, (2021).

[12] A. F. Putranto, M. Nur, A. Y. Wardaya, advances in physics theories and applications, vol. 71, 2225-0638, (2018).

[13] E. M. Lifshitz, L. P. Pitaevskii, Physical Kinetics, vol. 10, Elsevier, Amsterdam, (1995).

[14] K. MIYMOTO, plasma physic and controlled nuclear fusion, Tokyo, Japanese, university of Tokyo press, (2004).

[15] R. P. Drake, High Energy Density Physics, Springer, Library of Congress Control, Netherlands, (2006).

[16] H. K. Chug, R. W. Lee, M. H. Chen, Y. Ralchnko, http://nlt.nist.govL, 14 /12/ 2019, 11:00am.

[17] E. Tatarova, FM. Dias, E. Felizardo, J. Henriques, CM. Ferreira, Gordiets "Microwave Plasma torches driven by surface waves" PSST 17, (2008).

[18] E. Hnatiuc, D. Astanei, M. Ursache, B. Hnautiuc, "A Review over cold Plasma reactors and their applications" ICEPE, 497 – 502, (2012).

[19] A. Fridman, A. Gutsol, Y.I. Cho, advances in heat transfer, vol. 40, (2007).

[20] F. F. Chen, introduction to plasma physics and controlled fusion, 3rd edition, spring international, AG. Switzerland, (2016).

[21] B. Mouawad, ,M. Soueidan, D. Fabregue, C. Buttay, B. Allard, V. Bley, C. Martin, "Application of the spark plasma sintering technique to low-temperature copper bonding" IEEE Transactions on Components, Packaging and Manufacturing Technology, 553-560, 2, (2012).

[22] T. Anderson, Plasma Antennas, 2nd Edition, Artech House, America, (2021).

[23] A. Unsold, Die Physik der Sternatmosphären, Springer, Berlin, (1968).

[24] L. Biermann, Z. Astrophys. 29, 274, (1951).

[25] E. N. Parker, Ap. J. 128, 664 (1958).

[26] B. M. Smirnov, Physics of ionizeed gases, John Wiley & Sons, Inc, UK, (2001).

[27] D. Kondepudi, I. Prigogine, modern thermodynamics from heat engines to dissipative structures, second edition, John Wiley & Sons Ltd, United Kingdom, (2015).

[28] M.J. Oliveira, equilibrium thermodynamics, second edition, Springer, Berlin, Germany, (2017).

[29] M. D. Calzada, M. Moisana, A. Gamero, A. Sola, J. Appl. Phys. 80 (1), (1996).

[30] J. A. M. Van der Mullen, Phys. Rep. 191, 109, (1990).

[31] U. Fantz, basics of plasma spectroscopy, plasma sources Sci. Technol, 15, S137-S147, (2006).

[32] G. L. Sewell, reports on mathematical physics, vol. 72, No.3, (2013).

[33] H. W. Drawin, Z. Physik 228, 99–119, (1969).

[34] T. Fujimoto, R. W. P. McWhirter, phy. rev. A., vol. 42, No.11, (1990).

[35] Z. Xu-Tao, CHIN.PHYS.LETT. Vol. 22, No. 5, 1183, (2005).

[36] M. Belkhiri, thesis of doctorate, Paris Sud XI University, (2014).

[37] J. M. Gil, R. Rodriguez, R. Florido, J. G. Rubiano, P. Martel, E. Minguez, Laser and Particle Beams, USA, 26, 1–11, (2008).

[38] C. De Michelis, M. Mattioli. Soft-x-ray spectroscopic diagnostics of laboratory plasmas. Nuclear Fusion, 21(6), 677–754, (1981).

[39] F. de Gaufridy de Dortan, Etude de l'influence de l'environnement plasma sur les sections efficaces d'excitation collisionnelle electronion dans un plasma chaud et dense, PhD thesis, University Paris XI, (2003).

[40] M. Jullien, Spectroscopic analysis and numerical simulation of a photoionized neon plasma experiment, PhD thesis, University Paris Saclay, (2021).

[41] J. J. S. Shang, Aerospace, 5, 2, (2018).

[42] G. Herzberg, atomic spectra and stomic structure, 2nd ed, Dover Publisher, New York, USA, (1944).

[43] Y. P. Raizer, Gas Discharge Physics; Springer: Berlin, Germany, (1991).

[44] S. T. Surzhikov, J. S. Shang, J. Comput. Phys.,199, 437–464, (2004).

[45] T. M. York, H. B. Tang, introduction to plasma and plasma dynamics, Elsevier Inc, America, (2015).

[46] T. Ito, Y. Otani, N. Namiki, electrostatic separation of carbon dioxide by ionization in bifurcation flow, Aerosol and air quality research, vol. 4, No. 1, pp91-104, (2004).

[47] R. W. Lee, B. L. Whitten, R. E. Strout, J. Spectra-A model for K-shell spectroscopy "Quant. Spect. Radiat. Trans., 32, 91 (1984).

[48] M. Nakano, excitation energies and properties of open-shell singlet molecules, Springer, New York, (2014).

[49] C. A. Nicolaides, D. R. Beck, excited States in quantum chemistry, 1 st edition, NATO Scientific Affairs Division, U.S.A., Canada, (1979).

[50] M. Baudelet, in Laser Spectroscopy for Sensing, Elsevier, UK, (2014).

[51] I. I. Sobelman, atomic spectra, and radiative transitions, Springer-Verlag Berlin Heidelberg, New York, (1979).

[52] M. A. Baig, Atoms, 10, 39, (2022).

[53] J. A. R. Samson, Photoionization of atoms of and molecules, Physics reports, section C of Physics Letters, 28, No.4, 303–354, (1976).

[54] I. L. Bradeanu, photoionization, and excitation of free variable size Van Der Waals clusters in the inner shell regime, thesis of doctorate, Bayerischen Julius-Maximilians-University, Wurzburg, (2005).

[55] A. Safdar, Electron-ion recombination data for plasma applications, Stockholm University, Sweden, Stockholm, (2012).

[56] A. Lankin, G. Norman, Contrib. Plasma Phys. 53, No. 10, 711 – 720, (2013).

[57] A. V. Gurevich, L. P. Pitaevskil, SOVIET PHYSICS JETP, vol. 19, No., 4, (1964).

[58] J. Dubauf, S. Volonti, Rep. Prog. Phys., vol. 43, (1980).

[59] Z. Altun, A. Yumak, N. R. Badnell, S. D. Loch, M. S. Pindzola, A&A 447, 1165–1174, (2006).

[60] Z. Shotan, O. Machtey, S. Kokkelmans, L. Khaykovich, Phys. Rev. Lett. 113, 053202, (2014).

[61] S. X. Hu, Phy. Rev. Lett 98, 133201, (2007).

Chapter 2

Theoretical Aspects

2.1 Introduction

The atomic collision is a complex process. This interaction generates processes like elastic scattering, which predominates at low collision energies, excitation and ionization processes to bound and continuum states, electron exchange processes, and the coherent impact correlation phenomenon [1].

Over the past decades, the difficulties of producing charged ions due to electron impact ionization have been researched especially in relation to the development of plasma physics, controlled nuclear fusion, and heavy ion accelerators. Ion sources produce charged ions as a result of electron impact ionization of atoms or molecules, When an electron collides with a neutral particle, it may emit an electron with higher energy than the binding energy of the atom's respective electron. This electron is then transported to the spectrum of unbound states and lost by the molecule, implying that the electron has been ionized. The neutral atom becomes a charged ion as a result of this process [2].

The ionization of elements by electron impact is a beneficial process to determine the properties of nonequilibrium plasmas, which can be found in many branches [3].

Since Thomson's work in the early 1910s, the ionization of atoms by the impact of charged particles has been a subject of ongoing attention. Powell and Rudge have both published reviews on ionizing collisions including two free electrons in the end state, making their theoretical explanation of them much more challenging than collisions that excite the target atom to bound states [4].

In addition to that, through different impacts ionization coefficients, determine the most important physical plasmas' behaviors [5]. Furthermore, the atomic structure of elements consists of a positive nucleus with high density surrounded by one or more electrons in the orbital move. However, the electrons must have enough binding energy to hold them in different shells, for multi-electron atoms, the inner complex interactions with atoms influence the ionization process [6].

One of the main uses of ionization electron impact is the non-equilibrium ionized kinds whose concentrations must still satisfy to protect collective behavior, also the number of ionized kinds and the number of elementary reactions are greater in the study medium [7]. Also, the electron impact ionization cross sections for ions are relied on the modeling of hot plasmas, both laboratory, astrophysical and fusion plasma systems of the Tokamak devices Due to the difficulties of measuring or calculating electron ionization rates for ionized atoms, semiclassical and semiempirical estimates which are based on the finite amount of data available for neutral or singly charged systems [8].

Atomic molecule ionization by electron impact has the main role in plasma processes, mass spectrometry, atmospheric research, and other domains where the energetic ions in planets and some of their satellites are produced in large part by electron interactions with molecular species [9].

2.2 Cross sections

Electron-impact spectroscopy gives information about several energetically feasible processes (elastic scattering, excitation, ionization, dissociation, electron capture, etc.), and numerous combinations of these primary processes. The probability of the occurrence of those processes occurring is represented in terms of quantities called cross sections. The ionization state of a collisional plasma is defined by a balance of electron collisional ionization rates. Regardless of whether the plasma is in a stable or temporary state. Exceedingly, accurate knowledge of these rates is needed [10].

The importance of this scaling is that classically scaled ionization cross section plotted versus scaled energy varies slowly along an isoelectronic sequence, particularly at high values of the nuclear charge Z [11]. Several researchers have used a theoretical or empirical formula to determine the electron impact

ionization cross section. Where their aim of them is to describe a cross section of data with an expression containing a few parameters derived largely from the data [12].

2.2.1 Empirical Cross Sections

◇ Thomson cross section

The ionosphere was initially studied using observations from Thomson scattering. In 1958, Gordon proposed that the radiation emitted by free electrons may be detected by sending a beam of radio waves into the ionosphere at a frequency far higher than the plasma cutoff frequency. The electron density and temperature are determined by analyzing the spectra and scattered power. The fluctuation of the electron density affects the phenomenon of Thomson scattering in plasma. The total scattered power would be zero if the electrons were stationary and distributed at randomly because they are in thermal motion, and there are fluctuations in the density of electrons. Additionally, collective plasma effects happen and the ion fluctuations affect the electron fluctuations when the probing wave's wavelength is longer than the Debye length. Therefore the scattering is the result of an interaction between the incident wave, a wave vector, and a plasma thermally exciting wave [13].

The classical process of light being deflected by a charged obstruction of a typical size less than the wavelength of the incident radiation is known as Thomson scattering. Therefore, the Thomson cross section can be given as [14, 15, 16]:

$$\sigma_{Th} = \frac{P_{rad}}{S} \tag{2.1}$$

And, the radiated power is:

$$P_{rad} = \frac{2}{3}\frac{e^4}{4\pi m^2}E^2 \tag{2.2}$$

When you divide this by the energy flux, which is the modulus of the Poynting vector for a plane wave (PW)).

$$S = |\overrightarrow{E} \wedge \overrightarrow{B}| = E^2 \tag{2.3}$$

E is being the electric field, B is magnetic field, and Lorentz force is $(\overrightarrow{v} \wedge \overrightarrow{B})$.

◇ Born approximation

Leon Van Hove presented the pseudopotential depending on Fermi's assertion in 1954, where the effective potential is the base of the interaction between a neutron and a nucleus. On the other hand, the actual interaction potential is stronger than the pseudopotential interaction. Thus, the Born approximation is a perturbation expansion derived from enough weak pseudopotential interaction. Conversely, this approximation is close to the incident field as the driving field in scattering theory. The Born approximation is as small as the scattering field amplitude in comparison to the incident field amplitude [17].

In inverse scattering issues, the Born approximation is frequently employed to reduce computational complexity, but its validity and applicability are not clearly defined. The incident field serves as the scattering's overall field in the Born approximation [18].

In the Born approximation, the recommended cross section is given by the following equation [19]:

$$\sigma_{Born} = \frac{4\overline{\phi}}{k^3} \int_1^{k-1} \left(E_1^2 + E_2^2 + \frac{2}{3}E_1E_2\right)\left(\ln\frac{2E_1E_2}{k} - \frac{1}{2}\right)dE_1 \tag{2.4}$$

$(k \gg 1)$ is the energy where:

$$\overline{\phi} = \frac{e^2}{\bar{h}c}\left(\frac{Ze^2}{mc^2}\right)^2 = 5,7938.10^{-28}Z^2 \qquad (cm^2) \tag{2.5}$$

◇ Born-Bethe approximation

The Born approximation is extremely trustworthy in order to guarantee that the Bethe approximation behaves correctly at energies. Its statement is highly suited for use in investigating a particular transition for one or two optional energies in various modeling investigations [20].

In the Bethe-Born approximation the cross sections for ionization or excitation of atoms by high energy electrons [21]. The expression for the Born-Bethe cross section can be written as:

$$\sigma_{Bethe-Born} = \frac{8f}{E\Delta E}\pi a_0^2 \ln\frac{q_0}{k_0 - k_1} \tag{2.6}$$

And f is the oscillator strength of the transition $[0;1]$, a_0 is the radius of the first Bohr orbit of atomic hydrogen, q_0 is the cutting-off parameter, q_0 is the reasonable estimation, which is shown as:

$$q_0 = min\left(k_0 + k_1, \sqrt{2E_0}\right) \tag{2.7}$$

At high electron-impact energies $E \gg \Delta E$, Eq.2.6. Gives for the cross section:

$$\sigma = \frac{8f}{E\Delta E} \ln \frac{136E^{\frac{1}{2}}}{r_0 \Delta E} \pi a_0^2 \tag{2.8}$$

Where

$$k_0 \pm k_1 = \sqrt{2E}\left(1 \pm \sqrt{1 - \frac{\Delta E}{E}}\right) \tag{2.9}$$

The Bethe formula and its modifications are often used to estimate dipole excitation cross sections, but its accuracy is less than that of the Bron approximation [21].

◇ Belfast cross section

The global collection of suggested data on electron-impact ionization of various atoms and ions produced at the Queen's University of Belfast (Northern Ireland), stood out among a number of compilations of electron-impact ionization cross sections and recommended its analysis [22].

The recommended cross sections of Belfast have been Dtted by the so called BELI formula, the suggested cross sections are calculated using the formula below [23].

$$\sigma_{Belfast} = \frac{1}{IE}\left[A \ln \frac{E}{I} + \sum_{i=1}^{N} B_i \left(1 - \frac{I}{E}\right)^i\right] \tag{2.10}$$

Where E is the energy of the incident electron, I is the ionisation potential, A is a Bethe coefficient and determines the high energy behavior of the cross section. B_i are determined by a least squares convenable procedure.

$$A = \frac{I}{\pi a} \int_I^{\infty} \frac{\sigma_{ph}}{E} dE \tag{2.11}$$

wnere σ_{ph} isthe photoionization cross sectIon and a is the fine structure constant. they have evaluated the A coefficient for a number of the atoms and ions under investigation and this value has been incorporated in Eq. 2.10 to enable high energy extrapolation.

2.2.2 Semi - Empirical Cross Sections

◇ Electron-Impact Multiple-Ionization cross section (EIMI)

An electron - ion collision that produces the ejection of multiple electrons is known as electron-impact multiple ionization. In dynamic systems, the ions are abruptly exposed to greater electron temperatures, Therefore EIMI ought to be important for solar flares, nanoflare coronal heating, and supernova remnants. When such non-thermal distributions are found in astrophysical systems, EIMI is pertinent to the modeling of those systems. A representation of the EIMI crosse sections. It can be explained using the formula below [24, 25].

$$\sigma_{EIMI} = f \frac{p_0 p_1^{p_2}}{\left(E_{th} \diagup E_{Ryd}\right)^2} \left(\frac{u}{u+1}\right)^{p_3} \frac{\ln u}{u} .10^{-18} \tag{2.12}$$

Where $E_{Ryd} = 13.606$ eV, and $u = E_{th}$ is the incident electron energy E, normalized by the direct multiple-ionization threshold E_{th}. The parameters p_0 and p_2 rely on the number of the electron being removed and have been tabulated by Shevelko, Tawara, and Belenger et al. The parameter p_1 is the number of electrons in the target ion, and $p_3 = 1.0$ stands neutral targets or 0.75 stands ionic targets [24].

◇ Deutsch-M*ä*rk cross section (DM)

The Deutsch-M*ä*rk method has many advantages over other semiempirical approaches. Firstly, it is easier to apply and requires lesser semi-empirical parameters that are also easily related to physical quantities. Secondly, the energy-dependent function is derived from classical considerations is the same for all stages of ionization. The cross sections by the DM method of rare gases are used in the fitting technique for the computation of multiple atomic ionization cross sections to determine the relevant weighting factors empirically. However, it was discovered that this fitting approach could only be used for multiple ionizations when $m < 5$. Accurate rare gas ionization cross sections for higher ionization stages, $m > 5$ are insufficiently common to provide a

trustworthy fitting approach, and it is given as [26].

$$\sigma_{DM} = \sum_{n,l} g_{nl} \pi \left(r_{nl}\right)^2 \xi_{nl} f_l(U) \tag{2.13}$$

where g_{nl} is a weighting factor, ξ_{nl} is the number of electrons in the nl shell, $(r_{nl})^2$ is the mean square radius of the nl-shell, and the function $f_l(U)$ explains the energy dependence of the ionization cross section. Here, U is the reduced impact energy, denoted by the formula $U = E/E_{nl}$, where E is the incident electron's energy and E_{nl} is the binding energy of the electrons in the $n\ l$ shell.

◇ Lotz et al. cross section

Cross sections for electron impact ionization of ions and atoms are necessary for developing useful models for high-temperature plasmas and for analyzing diagnostic findings in such plasmas. Therefore the empirical formula that is developed by Lotz is being widely applied [22, 27].

Moreover, the kinetic energy E of the impacting electron is higher than the binding energy P_i of the bound electrons, and all atoms, ions, or electrons each contribute a little portion of the gross ionization cross-section. Besides, the subshell cross-section is produced equally by each comparable electron [28, 29]:

$$\sigma_{Lotz} = \sum_{i=1}^{N} a_i q_i \frac{\ln\left(E/P_i\right)}{E P_i} \left(1 - b_i exp\left[-c_i \left(\frac{E}{P_i} - 1\right)\right]\right); \quad E \geqq P_i \tag{2.14}$$

P_1 is the ionization potential; q_i is the number of equivalent electrons in the i-th subshell, a_i, b_i, and c_i, are individual constants, which have to be theoretically or experimentally determined, or through reasonable guesswork.

While, near threshold $E \approx P_1$, 2.14 becomes [28]

$$\sigma_{Lotz} \approx a_1 q_1 \frac{(E/P_1 - 1)}{P_1^2} (1 - b_1) \quad \infty \quad U - 1 \tag{2.15}$$

Where $U = \frac{E}{P_1}$.

In another case, eq. 2.14 changes when there are large electron energies $E \gg P_i$[29].

$$\sigma_i \approx a_i q_i \frac{\ln\left(E/P_1\right)}{E P_1} \quad \infty \quad \frac{\ln E}{E} \tag{2.16}$$

Also, the creation of practical models for high-temperature plasmas and the analysis of diagnostic controls, cross sections and rates for electron impact ionization of ions are necessary. Plasma modelers depend on relative or approximate ways of calculating rates. Lotz's semi-empirical formula is still commonly used. Hence, the classical scaling law allows that the Lotz formula to be prepared to replicate the available experimental data and detect cross sections for other atoms and ions [30].

◇ Arnaud et al. cross section

It is necessary to understand the ionization rate coefficients for various ions in order to comprehend ionization equilibrium in a laboratory setting and astrophysical plasmas. Numerous empirical equations have been proposed to calculate the cross section and coefficients of the ionization rate. Using the parametric formula proposed by Younger (1981a) for direct ionization and used by PGBYH for the theoretical cross section, Arnaud and Raymond changed the cross section for specific ions[31, 32].

$$\sigma_{Arnaud} = \sum_j \frac{1}{u_j I_j^2}\left[A_j\left(1-\frac{1}{u_j}\right)+B_j\left(1-\frac{1}{u_j}\right)+C_j\ln(u_j)+D_j\frac{\ln(u_j)}{u_j}\right] \quad (2.17)$$

Where the coefficients A_j, B_j, C_j, and D_j are constants, I_j is the ionization potential for the level j, and $u_j = \frac{E}{I_j}$.

◇ Monte Carlo simulation cross section (MC)

The Monte Carlo approach shows the transfer of the subsequent electrons ejected through ionization [33]. It is frequently used in collision physics from minimum to high projectile energies to calculate charge exchange, excitation, and ionization cross sections. When it comes to ionization processes in ion-atom collisions, the MC approach is very effective. Besides, in classical dynamics, all particle interactions may be precisely taken into account during the collision. This model is founded on the numerical integration of the conventional motion equations for the system under investigation [34].

There is also no limit on the number of particles and it is possible to observe all particle trajectories during the impact. At relatively large internuclear distances between the projectile and target atoms, a random ensemble representing the approximate quantum mechanical phase space distribution

for two distinct atoms is used to select the beginning circumstances. It took a lot of trials to get the simulations' level of uncertainty down. The following formula was used to calculate the total ionization cross section [34]

$$\sigma_{MC} = \frac{2\pi b_{max}}{T_N} \sum_{j=1}^{T_N^{(c)}} b_j^{(c)} \tag{2.18}$$

Where, T_N is the total number of computed trajectories with impact parameters below b_{max}, $T_N^{(c)}$ is the total number of trajectories that satisfy the requirements for the inquiry final channel, and $b_j^{(c)}$ is the trajectory's actual impact parameter and corresponds to the final channel under investigation.

2.2.3 Calculation Code

◇ EMPIRE-3.2 and TALYS-1.8 codes

The computer codes EMPIRE-3.2 and TALYS-1.8 are applied to simulate cross section data for light particle reactions. The codes extend detailed information on reaction cross sections based on several reaction mechanisms, such as direct reactions, preequilibrium emission, and compound nucleus processes [35].

For each mechanism, the code incorporates different nuclear models, such as a statistical theory of Hauser-Feshbach for the compound nuclear, an excitation model with PCROSS code for pre-equilibrium contribution, and ECIS06 code for calculating the transmission coefficient and direct reaction contributions using an appropriate optical model potential [35].

◇ PROTEUS code

The PROTEUS code can know multigroup cross sections in the ISOTXS format, that are generated offline with cross section generation codes or produce multigroup cross sections on the fly with a cross section library that includes isotropic cross sections and resonance parameters as a function of temperature and background cross section. In the case of the latter, cross-section application programming is used [36].

The CSAPI helps PROTEUS to read the cross section library, solve the stable source problems, interpolate cross sections utilizing temperature and background cross section, and create and assign multigroup cross sections for use

in PROTEUS. While, the CSAPI calculates multigroup cross sections for every region, taking into consideration temperature, energy, and spatial resonance self-shie [36].

◇ ATOM code

The ATOM program is utilized to calculate the many radial functions such as collisional features, rate of autoionization, cross sections for photo recombination, excitation, impact electron ionization, and other aspects of the interactions between photons and electrons in neutral atoms or positive ions. This code calculates the collisional and radiative characteristics of atoms and ions of charge, which has $Z \leq 99$, and the principal quantum number is $n \leq 9$. The ATOM algorithm is dependent on the semi-empirical electron approximation approach for radial wave functions of experimental values for the optical electron's energy as an input parameter. For each arbitrary transition. The ATOM code determines the collisional and radiative properties of atoms and ions, however with a principal quantum number n_1 of the high level limited: $n_1 \leq n_0 + 6$, where n_0 is the basic level [37].

◇ Modified HFR code

The simply excited wave functions depend on the modified HFR code from 1snl to the major quantum numbers n=30. Also, they are used is configuration interaction with high angular momentum states and increased numeric accuracy of mixing coefficients [38].

◇ Flexible Atomic Code (FAC)

There are computer programs for calculating atomic processes that use either non-relativistic approximations or entirely relativistic methods. However, The majority of them focus on the atomic structure and bound-bound systems, such as nonrelativistic configuration interaction codes [39].

The performance from these structure codes for bound state wave functions is used by several modern programs for processes. This case can lead to the user interface becoming hard as a result of the contact between various applications, making it impossible for people who aren't creators to use the codes actually. There are some integrated packages available for calculating atomic processes such as the ATOM package [40].

Meanwhile, the Flexible Atomic Code (FAC) is an advanced atomic package (GU 2002). which is a relativistic, multiconfigurational atomic code like HULLAC, and for all continuum systems, the distorted-wave (DW) approximation is used. Also, the isolated resonance approximation is a separate method that treats resonant processes like DR and RE [32].

The formula for the DW electron impact ionization cross section differential in the energy of the ejected electron may be obtained from that for electron impact excitation (EIE) by replacing one bound orbital in the final state with the free orbital of the ejected electron and summing over its angular momentum. It can be expressed in terms of the collision strength similar to that of EIE.

$$\sigma(E_0, E) = \frac{1}{E_0^2 g_0}\Omega_{01} \tag{2.19}$$

Where E_0 and k_0 are the energy and kinetic momentum of the incident electron, E is the energy of the ejected electron, g_0 is the statistical weight of the initial state. The collision strength Ω_{01} is:

$$\Omega_{01} = 2 \sum_{\kappa, J_T, k, a_0\beta_0} Q^k(a_0\kappa;\beta_0\kappa)\langle\psi_0 \parallel Z^k(a_0,\kappa) \mid \psi_1,\kappa;J_T\rangle \langle\psi_0 \parallel Z^k(\beta_0,\kappa) \mid \psi_1,\kappa;J_T\rangle \tag{2.20}$$

where κ is the relativistic angular quantum number of the ejected electron, J_T is the total angular momentum of the final state coupled with the ejected electron, the radial part Q_k is identical to that for EIE, except that one of the bound orbitals in the final state is now replaced by a free orbital. Note that Q_k contains the summation over the partial waves of the incident and scattered electrons.

And

$$k_0^2 = 2E_0\left[1 + \frac{a^2}{2}E_0\right] \tag{2.21}$$

where a is the fine structure constant.

Substituting this into 2.20 and after carrying out the summation over J_T analytically becomes:

$$\Omega_{01} = 2 \sum_{\kappa, a_0\beta_0} \delta_{j_{a_0} j_{\beta_0}} [j_{a_0}]^{-1} \overline{Q}^k(a_0,\beta_0)\langle\psi_1 \parallel \tilde{a}_{\tilde{a}_0} \parallel \psi_0\rangle\langle\psi_1 \parallel \tilde{a}_{\tilde{\beta}_0} \parallel \psi_0\rangle \tag{2.22}$$

Where $\overline{Q}^k(a_0, \beta_0) = \sum_k Q^k(a_0\kappa, \beta_0\kappa)$. Note that since only basis states with the same parity can mix, the condition $j_{a_0} = j_{\beta_0}$ implies that $l_{a_0} = l_{\beta_0}$ as well. Therefore, if the configuration interaction is limited within the same n complex, only terms with $a_0 = \beta_0$ survive in the summation.

The total ionization cross section is obtained by integrating Ω_{01} over the energy of the ejected electron E.

$$\sigma(E_0) = \int_0^{(E_0-I)/2} \sigma(E_0, E)dE \tag{2.23}$$

Where I is the ionization energy. The ionization energy enters the radial integral Q_k implicitly, since $E_0 = I + E_1 + E$, where E_1 is the energy of the scattered electron [32].

2.3 Distribution Functions

Functions resemble specific types of vectors. Such as $f(x)$ that collects one set of numbers (the "argument", x, of the function), to another (result or value). The main idea remains the same for functions that have numerous variables, complex values, or geometric vector results (such as a position or momentum vector). Besides, the set of possible values for the argument can be thought of as a list of integers, and they can be thought of as another list [41].

It is commonly known that the quantum mechanical idea of phase space is troublesome due to the uncertainty principle. One cannot define a probability that a particle has a position and a momentum, or an exact phase space probability distribution for a quantum particle, because a particle cannot simultaneously have a well-defined position and momentum. However, distribution functions look like phase space distribution functions, and they are interesting to quantum mechanical systems. In addition, they can also show the relationships between classical and quantum mechanics [42].

2.3.1 Maxwell distribution function

The Maxwell distribution is a fundamental distribution in statistical mechanics [43], in addition to being widely used in statistics for modeling lifespan data, it is frequently employed to predict the speed of molecules. The Maxwell Boltzmann distribution is another name for the Maxwell distribution. It bears the names of Ludwig Boltzmann and James Clark Maxwell. It is renowned for

its usefulness in many scientific fields, including astrophysics, chemistry, and engineering [44].

By using a distribution function, Maxwell characterizes the state of a gas based on two conditions. Firstly, the function must reflect isotropy and be spherically symmetric. Secondly, in order to reflect the independence of the three coordinate directions, the velocity components should be separable. He also demonstrated that collisions do not alter his distribution without making reference to his two initial conditions. Besides, Boltzmann demonstrated that the Maxwellian is only the most likely distribution in an isolated system with a given particle number and a given energy. It is accurate to say that a group of particles is defined by the Maxwellian distribution is in thermal equilibrium which is a super approximation for rarefied gases at moderate temperatures [45, 46].

In the other hand, distribution functions, $f(E)$ of the distribution are given by the concept of temperature is only valid for a Maxwellian distribution, which is written as [47]:

$$f_M(E) = \frac{2\sqrt{E}}{T^{\frac{3}{2}}\sqrt{\pi}} exp\left(\frac{-E}{T}\right) \tag{2.24}$$

2.3.2 Non-Maxwellian distribution function

A renewed interest in distribution functions and the spectrum of the alpha particles produced in spin-polarized plasma by nuclear reactions which have recently demonstrated the significance of non-Maxwellian distributions in a variety of fields of physics, including nuclear astrophysics, solar neutrino problems, cooling techniques in particle accelerators, and nuclear reactions. Many times, the many-body interactions among the free particles of the distribution can be used to justify non-Maxwellian distributions. When describing phenomena like neutrino generation and transport to the sun's surface, these effects in nuclear astrophysics are crucial. In the first approximation, the average Coulomb interaction of the individual particles in the distribution might be superimposed on an external, average field to characterize the many-body effects [48].

Additionally, non-Maxwellian distribution functions are frequently observed in space and laboratory plasmas in quasi-stationary states. They usually result from long-range nonlinear wave-particle interactions [49], which can't be a

source of stability and create a variety of electrostatic and electromagnetic waves [50].

When the hot electrons are interesting in plasma and in order to be detected into the main mechanisms, non-Maxwellian presents an energy distribution function given by [51]:

$$f_{NM} = (1 - f_{hot}) f_M(T_{bulk}) + f_{hot} f_M(T_{hot}) \tag{2.25}$$

f_M the Maxwell energy distribution function, f_{hot} is the normalized hot electron fraction, and T_{hot} and T_{bulk} are the hot and bulk electron temperature, respectively.

2.3.3 Gaussian distribution function

The most significant distribution in statistics is the Gaussian distribution, this continuous probability distribution roughly characterizes a group of objects with a focus on their mean. The bell-shaped probability density function has a mean peak. The central limit theorem, which states that the average of a large number of independent random variables with identical distributions is roughly Gaussian distributed, which is another factor that contributes to its popularity [52].

Gaussian distribution functions are preferred over other symmetrical statistical distribution functions because they use as a reference for all others.
Clearly, deviations from the norm are easily visible and may contain useful information. It also has well established mathematical features. Therefore, its distribution function has the next form [53]:

$$f_G(x) = \frac{1}{\sqrt{2\pi\sigma}} exp\left(-\frac{(x-\mu)^2}{2\sigma}\right) \tag{2.26}$$

Where x is the independent variable, μ is the expectation of the independent variable, and σ is the variance.

2.3.4 Power Law distribution function

The power law distribution has gotten a lot of attention over the years because of its mathematical features, which can lead to unexpected physical implications, as well as its manifestation in a wide spectrum of natural and physical phenomena. In addition to this, the distribution applies only to values

greater than a certain minimum in empirical phenomena. The tail of the distribution is said to realize a power law in such instances [54].

The power law distribution functions that have a negative exponent ($-\alpha(\alpha > 1)$). The sign is detached from the absolute value. Also, the exponent is parametrized by the minimum and maximum border (x_{min}, x_{max}). The cumulative distribution function is given by [55]:

$$f_{PL}(x) = \frac{x^{1-\alpha} - x_{min}^{1-\alpha}}{x_{max}^{1-\alpha} - x_{min}^{1-\alpha}} \tag{2.27}$$

The family of this distribution is presented by the precedent equation contains the 'unlimited' or 'not truncated' distributions with infinite upper limit ($f(x_{max} = \infty)$), which is famous in the (non-astronomical) literature as the Pareto distribution.

2.3.5 The Log-Normal distribution function

The log-normal distribution is a common model of the asymmetric distribution [56]. Furthermore, the most used model is positive modeling along with right-skewed continuous data [57].

Besides, deforming the normal distribution yields the log-normal distribution. Because the q-Gaussian distribution is an extension of the normal distribution, it is natural to think of it as a distribution with similar distortion, and its use would help analyze data from real-world occurrences more precisely. Where x is distributed as the log-normal distribution of a parameter (μ, σ^2), if $\log x$ is distributed as the normal distribution. Then, f_{LN} is given by [58]:

$$f_{LN}(x) = \frac{1}{\sqrt{2\pi}x\sigma} exp\left[-\frac{(\log x - \mu)^2}{2\sigma^2}\right] \tag{2.28}$$

Where

$$0 < x < \infty$$

2.4 Superstatistics distribution

Statistical superposition considers a modern try to formulate a statistical mechanical distribution of unusual systems as the systems have a fluctuating temperature [59]. For this aim, Cohen and Beck accomplished new statistics, named superstatistics (in 2003), these depend on the ordinary Boltzmann

statistics, the latter is formed as a tool for studying systems with complex dynamics and nonequilibrium [60].

2.4.1 Superstatitics: definition

In non-Boltzmann-Gibbs distribution where the systems are out of equilibrium and non-extensive, The superstatistics displays a relative motion to explain gaining of it [61]. This statistic supposes the superposition of canonical ensembles at different temperatures [62]. Superstatistics is a section of statistical mechanics that appears in nonequilibrium and stable states with intensive parameters fluctuations [63]. Both Cohen and Beck named "superstatistics" because the new statistics is a type of "statistics of statistics" [64].

One can tell that superstatistics systems are superpositions of two (or more) unlike other statistics: one is given by ordinary Boltzmann factors, and the other by large-scale fluctuations of one (or many) intensive parameters(e.g. the inverse temperature) [65], Since then, it has served as a useful method for describing a wide range of dynamic structures with changing environmental conditions [66].

2.4.2 Superstatistic: principle

The superstatistics concept has been considered as an important way to describe common classes of complex systems [67]. The term of new statistics was coined and popularized in statistical thermodynamics a few years ago by Beck and Cohen, in order to model non-Maxwell Boltzmann statistical distribution in college nonequilibrium systems [68].

To have the superstatistics' main idea, consider a nonequilibrium with a long term stationary system [69], which is classified into many cells which are all small, and they are characterized by temperature's inverse value (Figure. 2.1). Another way, The system deals with the summation of local canonical ensembles [70].

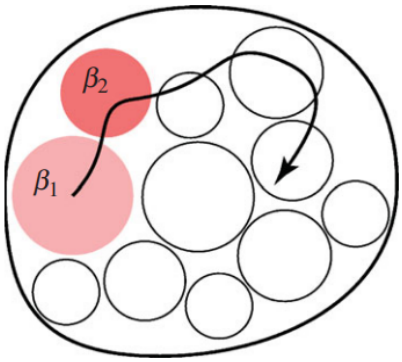

Figure 2.1: A spatially inhomogeneous situation of mesoscopic systems (sketched as circles) embedded into a fluctuation environment with different inverse temperatures bi. A Brownian particle moves through the different regions with different inverse temperatures [67].

This new kind depends on ordinary statistical mechanics, where it is described by ordinary Boltzmann factor ($e^{-\beta E}$). Thus, One may define an effective Boltzmann factor $B(E)$ for full system, namely [71]:

$$B(E) = \int_0^\infty f(\beta) e^{-\beta E} d\beta = \langle e^{-\beta E} \rangle \tag{2.29}$$

Where:

- $f(\beta)$ is the normalized probability distribution.
- E is an effective energy in each cell.
- $\beta = \frac{1}{K_B T}$ is approximately constant equal.

On the other hand, Eq 2.29 depends on the main hypothesis, which is that large groups of dynamically complicated systems with fluctuations have physical relevance for generalized Boltzmann factors. At the same time, there is a specific standard that must be realized by probability density, with [64]:

$$f(\beta) = \delta(\beta - \beta_0) \tag{2.30}$$

Where, β_0 is average of β

It is obvious that the Laplace transform of the probability density $f(\beta)$ provides the generalized Boltzmann factor of superstatistics. There are an infinite number of possibilities, but certain requirements must be met, greatly reducing the number of physically pertinent cases:

- $f(\beta)$ must be a normalized probability density, It may be a physically relevant density from statistics, as Gaussian, uniform…etc. However, other, as yet unidentified, distributions might be considered if the underlying dynamics are sufficiently complex. [72].
- The new statistics are reduced to Boltzmann-Gibbs statistics when there are no fluctuations of intensive quantities at all [73].
- The new statistics have to be normalized [74]:

$$\int_{-\infty}^{+\infty} f(\beta) d\beta = 1 \tag{2.31}$$

2.4.3 Type of superstatistics

There are two various types of superstatistics, They are known as the following [37].

- Type-A superstatistics

One normalizes this effective Boltzmann factor and obtains the stationary long-term probability distribution [75]:

$$P(E) = \frac{1}{Z(\beta)} B(E) \tag{2.32}$$

Where [37].

$$Z(\beta) = \int_{0}^{+\infty} B(E) dE \tag{2.33}$$

- Type-B superstatistics

For the sake of accuracy, Beck referenced it out that equation in type A is not properly normalized, And that a better way of writing it should be [76]:

$$P(\beta) = \int \frac{e^{-\beta E}}{Z(\beta)} f(\beta) d\beta \tag{2.34}$$

Besides, where $Z(\beta)$ is the $e^{-\beta E}$ normalization constant for a particular. By creating a new probability density $\tilde{f}(\beta) = cf(\beta)/Z(\beta)$, where c is a normalization constant, both methods can be simply transferred onto one another. It is clear that type-B superstatistics with f and type-A superstatistics with f are equivalent.

2.4.4 Superstatitics models

The invariant measure of the underlying dynamical system and an a priori nameless finally determine the distribution $f(\beta)$. One of the simplest $f(\beta)$ would be produced by Gaussian fluctuations, but these kinds of models are unphysical because they are negative with some nonzero probability, and they are required distributions, where β is always positive [64].

◇ Gamma distribution (χ^2 - distribution)

χ^2 -distribution also is known as Tsallis statistics [77], The Gamma distribution is created if the fluid can be represented by n independent Gaussians, X_i= $1, 2 \ldots n$, all with mean zero, Thus; That with $\beta = \sum_{i=1}^{N} X_i^2$; and $f(\beta)$ is known [78]:

$$f(\beta) = \frac{1}{\Gamma(\frac{n}{2})}\left(\frac{n}{2\beta_0}\right)\beta^{\frac{n}{2}-1}e^{-\frac{n\beta}{2\beta_0}} \tag{2.35}$$

In a more schematic form:

$$f(\beta) = \frac{1}{b\Gamma(c)}\left(\frac{\beta}{b}\right)\beta^{c-1}e^{-\frac{\beta}{b}} \tag{2.36}$$

With: $c = \frac{n}{2} > 1$; $b = \frac{2\beta_0}{n}$

Here Γ: Tsallis statistics function, n: number of freedom's degree.

Form the last two equations follow for the mean $\langle\beta\rangle$ and the variance σ^2 of $f(\beta)$ the expressions:

$$\langle\beta\rangle = bc = \beta_0 \tag{2.37}$$

And

$$\sigma^2 = \langle\beta^2\rangle - \langle\beta\rangle^2 = b^2c = \frac{2\beta_0^2}{n} \tag{2.38}$$

One gets then immediately, That in particular Tsallis' parameter q (entropic index of nonextensive statistical mechanics) can be explained as [78]:

$$\frac{1}{q-1} = \frac{n}{2} \Longleftrightarrow q = 1 + \frac{2}{n} \tag{2.39}$$

While

$$b = \frac{q-1}{\beta_0} \tag{2.40}$$
$$\langle\beta\rangle = \beta_0(mean)$$

Therefore

$$\sigma^2 = (q-1)\beta_0^2 \tag{2.41}$$

With a finite number of degrees of freedom (n) and a fluctuating environment, the gamma distribution is created quite naturally, The generalized Boltzmann factor is produced by the integration over β [64].

$$B(E) = \int_0^\infty f(\beta)e^{-\beta E}d\beta = (1+bE)^{-c} \tag{2.42}$$

Alternatively, the logarithm is expanded for tiny bE and written $B = e^{c\log(1+bE)}$. The outcome may be expressed in the form [64].

$$B(E) = e^{-\beta_0 E}(1 + \frac{1}{2}(q-1)\beta_0^2E^2 - \frac{1}{3}(q-1)^2\beta_0^3E^3 + ...) \tag{2.43}$$

◇ Log-normal distribution

β can be created by multiplicative processes. By virtue of the central limit theorem, for a large number of the microscopic random variables, The researched sum of their logarithms follows a Gaussian distribution [79]. Therefore, in a Log-normal distribution of β [64]:

$$f(\beta) = \frac{1}{\sqrt{2\pi}\beta s}e^{\frac{-\log\left(\frac{\beta}{m}\right)^2}{2s^2}} \tag{2.44}$$

Where, s, m are parameters.

The average is given by $\beta_0 = m\sqrt{w}$, while the variance of log-normal distribution is presented as $\sigma^2 = m^2w(w-1)$, and $w := e^{s^2}$

Therefore,

$$B(E) = e^{-\beta_0 E}(1 + \frac{1}{2}m^2w(w-1)E^2 - \frac{1}{6}m^3w^{\frac{3}{2}}(w^2-3w+2)E^3 + \ldots) \tag{2.45}$$

◇ Uniform distribution

A uniform distribution $f(\beta)$ of parameter $\beta > 0$ on some interval $\beta \in [a; a+b]$ is shown:

$$f(\beta) = \frac{1}{b} \tag{2.46}$$

Eleswhere: $f(\beta) = 0$, this distribution has a mean $\beta_0 = a + \frac{b}{2}$. And variance:

$$\sigma^2 = \langle \beta^2 \rangle - \langle \beta \rangle^2 = \frac{b^2}{12} \tag{2.47}$$

Uniform distribution's superstatistics is concluded from the generalized Boltzmann factor:

$$B(E) \approx \left[1 + \frac{1}{24}(bE)^2\right] e^{-\beta_0 E} \tag{2.48}$$

Where the effective Boltzmann factor ($B(E)$) follows from low energy reduction of the generalized Boltzmann factor. The superstatistics of the uniform distribution reduces to ordinary statistics when $b \longrightarrow 0$ [80].

◇ 2 - Level distribution

Suppose the subsystem can switch between two different discrete values of the temperature, each with equal probability; Thus, the probability density is defined by [64]:

$$f(\beta) = \frac{1}{2}\delta(a) + \frac{1}{2}\delta(a+b) \tag{2.49}$$

The average of β is given as: $\beta_0 = a + \frac{b}{2}$

And the variance one obtains:

$$\sigma^2 = \langle \beta^2 \rangle - \langle \beta \rangle^2 = \frac{b^2}{4} \tag{2.50}$$

While, the generalized Boltzmann factor is:

$$B(E) = \frac{e^{-\beta_0 E}}{2}\left[e^{\frac{bE}{2}} + e^{-\frac{bE}{2}}\right] \tag{2.51}$$

This is normalized for any $E \geq 0$.

For small (bE) one obtains:

$$B(E) = e^{-\beta_0 E}(1 + \frac{b^2E^2}{8} + \frac{b^4E^4}{384} + \ldots) \tag{2.52}$$

◇ F-distribution

In this distribution, one is taken into account a $\beta \in [0;\infty]$ distributed using therefore [64]:

$$f(\beta) = \frac{\Gamma(\frac{v+w}{2})}{\Gamma(\frac{v}{2})\Gamma(\frac{w}{2})}\left(\frac{bv}{w}\right)^{\frac{v}{2}} \frac{\beta^{\frac{v}{2}-1}}{(1+\frac{vb}{w}\beta)^{\frac{v+w}{2}}} \tag{2.53}$$

Where, v and w are positive integers, and $b > 0$ is a parameter. For $v = 2$, it obtains a Tsallis distribution. However, this is a Tsallis distribution in β-space, not in E-space.
The average is shown as: $\beta_0 = \frac{w}{b(w-2)}$

Besides, the variance:

$$\sigma^2 = \frac{2w^2(v+w-2)}{b^2v(w-2)^2(w-4)} \tag{2.54}$$

And the Boltzmann factor is written in the form:

$$B(E) = e^{-\beta_0 E}\left[1 + \frac{w^2(v+w-2)}{b^2v(w-2)^2(w-4)}E^2\right] + \\ - e^{-\beta_0 E}\left[\frac{4w^3(v+w-2)(2v+w-2)}{3b^3v^{\frac{3}{2}}(w-2)^3(w-4)(w-6)}E^3 + \ldots\right] \tag{2.55}$$

The generalized Boltzmann factor has a simple shape of the last distributions of superstatistics, which depends on the universal parameters q and β_0, it would look like this [64]:

$$B(E) = e^{-\beta_0 E}\left(1 + \frac{1}{2}(q-1)\beta_0^2E^2 + g(q)\beta_0^3E^3 \ldots.\right) \tag{2.56}$$

Here, $g(q)$ are presented by:

$$g(q) = 0 \qquad \text{(uniform and 2-level)} \tag{2.57}$$

$$= -\frac{1}{3}(q-1)^2 \qquad \text{(Gamma)} \tag{2.58}$$

$$= -\frac{1}{6}(q^3 - 3q + 2)^2 \qquad \text{(log-normal)} \tag{2.59}$$

$$= -\frac{1}{3}\frac{(q-1)(5q-6)}{3-q} \qquad \text{(F-distribution with v = 4)} \tag{2.60}$$

At last, there are some theoretical developments of the superstatistics concept containing the following; first, they prove a superstatistical generalization of fluctuation theories. Then, they define generalized entropies for general superstatistics. Additionally, superstatistics can relate to the fractional reaction equation, and superstatistical have path integral. On other hand, they may apply to cosmic ray statistics and hydroclimatic fluctuations [81].

2.5 The ionization rates coefficients

The modeling of thermonuclear fusion plasma allows rates coefficients for electron-impact excitation autoionization, direct ionization, recombination processes, and other atomic processes [82].

There are basically two methods through which ionization is brought on by electron collisions with neutral and ionized substances happens. The first is direct ionization, in which the collision causes a bound electron to become a free electron. It is common to refer to the second process as "excitation-autoionization". An autoionizing state of a bound electron is excited in this instance. A stabilizing radiative transition and an autoionizing transition are currently competing with one another. With isoelectronic sequencing, the relative contributions of the two processes can change significantly. Direct ionization predominates for the hydrogen through neon isoelectronic sequences. Excitation-autoionization is frequently the predominant ionization method for more complicated ions [11].

The ionization state of a collisional plasma is defined by a balance of electron collisional ionization rates. Regardless of whether the plasma is in a stable or temporary state. exceedingly, accurate knowledge of these rates is needed [11].

The rates coefficients (τ) are defined by uniting an energy dependent collision cross section of the electron energy distribution function [83, 84]:

$$\tau = \int_{\Delta E}^{\infty} v\sigma(E)f(E)dE \qquad (cm^3s^{-1}) \tag{2.61}$$

Where v is the velocity of electrons, $f(E)$ is velocity distribution of electrons function, and σ is the collisional cross-section.

2.6 Conclusion

In this chapter, we exposed empirical, semi-empirical, and calculation codes of cross sections, then distribution functions. We have also discussed superstatistics distribution. Finally, the ionization rates coefficients are presented.

References

[1] A. Chaudhry, H. Kleinpoppen, analysis of excitation and ionization of atoms and molecules by electron impact, Springer, New York, (2011).

[2] J. T. Tate, P. T. Smith, Phys. Rev., 39 (2), 270-277, (1932).

[3] L. J. Kieffkr, G. H. Dunn, REVIEWS Of MODERN PHYSICS, Vol. 38, No. 1, (1966).

[4] X. Llovet, C. J. Powell, F. Salvat, A. Jablonski, J. Phys. Chem. Ref. Data, vol. 43, No. 1, (2014).

[5] H. Ehrhardt, J. Roder, RECENT ABSOLUTE (e,2e) Measurents on atomic hydrgen and helium at low and intermediate energies, Coincidence Studies of Electron and Photon Impact Ionization, Edited by Whelan and Walters, Plenum Press, New York, (1997).

[6] H. Niwa, J. Suda, T. Kimoto, Impact Ionization Coefficients in 4H-SiC Toward Ultrahigh-Voltage Power Devices, IEEE TRANSACTIONS ON ELECTRON DEVICES, 62(10), 3326-3333,(2015).

[7] J. J. S. Shang, modeling plasma via electron impact ionization ,Aerospace, 5 (2), (2018).

[8] S. M. S. M. YOUNGER, Quant Spectrosc Radial Trans.fer Vol 27, No 5, Printed in Greal Britain, pp 541-544, (1982).

[9] U. R. Patel, K. N. Joshipura, Journal of Engineering and Technology, vol. 6, 2249 – 6157, (2013).

[10] H. Tanaka, M. J. Brunger, L. Campbell, H. Kato, M. Hoshino, A. R. P. Rau, Rev. Mod. Phys., Vol. 88, No. 2, (2016).

[11] K. P. Dere, Ionization rate coefficients for the elements hydrogen through zinc, A&A 466, 771–792 (2007).

[12] S. M. Younger, T D. Mark, Semi-Empirical and Semi-Classical Approximations for Electron Ionization, Springer-Verlag Wien, (1985).

[13] R. G. Seasholtz, NASA TN D-6372, Washington, (1971).

[14] J. Schwinger, L. L. Deraad, Jr., K. A. Milton, W. y. Tsai, Classical Electrodynamics, Westview Press, Boulder (CO), (1998).

[15] J. J. Thomson, Phil. Mag., Ser. 6, 6, 673 (1903).

[16] H. Bindslev, On the Theory of Thomson Scattering and Reflectometry in a Relativistic Magnetized Plasma, Ris-R-663(En), (1992).

[17] J. T. Cremer, Advances in Imaging and Electron Physics, vol. 173, 167–274, (2012).

[18] J. Li, X. Wang, T. Wang, Progress In Electromagnetics Research, vol. 107, 219–237, (2010).

[19] L. C. Maximon, Journal Of Research Of The Notional Bureau of Standards B. Mathematical Sciences, vol. 72B, No. 1, (1968).

[20] R. M. Abdul Hassan, A. A. Khalaf, Basrah Journal of Science, Vol. 37(2), 153- 162, (2019).

[21] B. L. Schram, L. Vriens, cross section formulae for ionization and excitation of atoms by high energy electrons, Physica 31, 1431-1436,(1965).

[22] K. L. ·Bell, H. B. Gilbody, J. G. Hughes, A. E. Kingston, F. J. Smith, J. Phys. Chern. Ref. Data, Vol. 12, No.4, (1983).

[23] A. L. Godunov, P. B. Ivanov, Physica Scripta. Vol. 59, 277È285, (1999).

[24] M. Hahn, A. Muller, D. W. Savin, The Astrophysical Journal, 850(2), 122pp, (2017).

[25] V. P. Shevelko, H. Tawara, NIFS-DATA-28, (1995).

[26] H. Deutsch, K. Becker, D. P. Almeida, T. D. M*ä*rk, international Journal of Mass Spectrometry and Ion Processes, 171, 119-126 (1997).

[27] T. Kato, K. Masai, M. Arnaud, NIFS-DATA-14, (1991).

[28] W. Lotz, Z. Physik, 206, 205-211, (1967).

[29] W. Lotz, Z. Physik, 216, 241- 247, (1968).

[30] M. A. Lennon, K. L. Bell, H. B. Gilbody, J. G. Hughes, A. E. Kingston, M. J. Murray, F. J. Smith, J. Phys. Chern. Ref. Data, Vol. 17, No.3, (1988).

[31] M. Arnaud, J. Raymond, Astrophysical J. 398,394–406, (1992).

[32] M. F. Gu, Astrophysical J. 582,1241–1250, (2003).

[33] B. Gervaisa, M. Beuveb, G.H. Oliverac, M.E. Galassi, Radiation Physics and Chemistry, 75, 493–513, (2006).

[34] S. J. Al Atawneh, O. Asztalos, B. Szondy, G. I. Pokol, K. Tokesi, Atoms, 8, 31, (2020)

[35] A. Gandhi, A. Sharma, Yu. N. Kopatch, N. A. Fedorov, D. N. Grozdanov, I. N. Ruskov, A. Kumar, Journal of Radioanalytical and Nuclear Chemistry, (2019).

[36] C. Lee, Y. S. Jung, Generation of the Cross Section Library for PROTEUS, ANL/NE-18/2, (2018).

[37] V. P. Shevelko, L. A. Vainshtein, Atomic Physics for Hot Plasma, IOP Publishing, UK, (1993).

[38] U. Fano , J. Phys. B, At. Mol. Phys., 7, 1401, (1974).

[39] A. Hibbert, A., Comp. Phys. Comm., 9, 141 (1975).

[40] M. Y. Amusia, L. V. Chernysheva, Computation of Atomic Processes: A Handbook For ATOM Programs, Institute of Physics Publishing, Bristol, (1997).

[41] D. A. B. Miller, Quantum Mechanics for Scientists and Engineers, Cambridge university press, New York, USA, (2008).

[42] M. Hillery, R.F. O'Connell, M.O. Scully, E.P. Winer, Physics Reports, 106, No. 3, 121—167, (1984).

[43] H. Krishna, M. Malik, Journal of Statistical Computation and Simulation, vol. 82, No. 4, 623–641, (2012).

[44] S. S. Bisht, C. Prakash, Journal of Scientific Research, vol. 65, No. 5, (2021).

[45] D. Moseev, M. Salewski, Phys. Plasmas 26, 020901 (2019).

[46] L. Zaninetti, International Journal of Astronomy and Astrophysics, 10, 191-202, (2020).

[47] E. Dzifcakova, Solar Physics 140: 247-267, (1992).

[48] G. Kaniadakis, P. Quaratia, Physica A, 192, 677-690, (1993).

[49] D. S. Oliveira, R. M. O. Galvao, PHYSICS OF PLASMAS 25, 102308 (2018).

[50] D. B. Graham , Y. V. Khotyaintsev, M. Andre , A. Vaivads, A. Chasapis, W. H. Matthaeus, A. Retino , F. Valentini, D. J. Gershman, Journal of Geophysical Research: Space Physics, 126, e2021JA029260, (2021).

[51] A. Escarguel, F.B. Rosmej, C. Brault, Th. Pierre, R. Stamm, K. Quotb, Plasma. Phys. Control. Fusion, 49, 85 (2007).

[52] X. Zhang, Gaussian Distribution. Encyclopedia of Machine Learning and Data Mining, 1–5, (2016).

[53] J. L. Bersillon, F. Villieras, F. Bardot, T. Gorner, J.M. Cases, J. Colloid and Interface Science 240, 400–411 (2001).

[54] A. Clauset, C. R. Shalizi, M. E. J. Newman, Power-Law distributions in empirical DATA, SIAM REVIEW, vol. 51, No. 4, pp. 661–703, (2009).

[55] T. Maschberger, P. Kroupa, Mon. Not. R. Astron. Soc. 395, 931–942 (2009).

[56] E. Crow, K. Shimizu. Lognormal Distribution. New York, NY: Marcel Dekker, (1988).

[57] A. Gardini, C. Trivisano, E. Fabrizi, Biometrical Journal, (2020).

[58] K. I. Koike, Y. Shimegi, On Log-q-Gaussian Distribution, Calcutta Statistical Association Bulletin, 70(2) 105–121, (2018).

[59] T. Yamano, thermodynamical and informatical structure of superstatistics, progress of theoretical physis supplement, No. 162, (2006).

[60] K. Ourabah, L. A. Gougam, M. Tribeche, PHYSICAL REVIEW E 91, 012133 (2015).

[61] H. Loguercio, D. Gonzalez, S. Davis, AIP. Conf. Proc, 1757, 060001-0600094,(2016).

[62] H. Loguercio, S. Davis, Journal of physics: conference series 720, 012007(2016).

[63] S. Sargolzeipor, H. Hassanabadi, W. S. Chung, Eur. Phys. J. Plus, 133:125, (2018).

[64] C. Beck, E. G. D. Cohen, physica A322, 267-275, (2003).

[65] C. Beck, physica A 342, 139-144, (2004).

[66] G. C. Yalcin, C. Beck, Physics Letters A 376, 2344–2347, (2012).

[67] C. Beck, Phil. Trans. R. Soc. A, 369, (2011).

[68] F. Sattin, Phys. Lett A, vol. 1. 240, (2018).

[69] A. M. C. Souza, C. Tsallis, Physica A, 342, 132138, (2004).

[70] S. Abe, Cent. Eur. J. Phys, 7(3), 401-404, (2009).

[71] H. Touchette, C. Beck, Physical Review E 71, 01131, 1-6, (2005).

[72] A. Boumali, F. Serdouk, S. Dilmi, Physica A, 124207(2020).

[73] S. Sargolzaeipor, H. Badi, W. S. Chung, Eur. Phy. J. Plus, 133:5, (2018).

[74] C. Tsallis, A. M. C. Souza, Phys. Rev. E 67, 026106 (2003).

[75] C. Beck, Continuum Mech. Thermodyn. 16: 293–304, (2004).

[76] F. Sattin, Eur. Phys. J. 349, 219-224 (2006).

[77] P. Rabassa, C. Beck, physica A, 417, 18-28, (2015).

[78] E. G. D. Cohen, superstatistics, Physics D, 193, 35-52, (2004).

[79] K. Ourabah, Eur. Phys. J. Plus, 135-136, (2020).

[80] U. S. Okorie, A. N. Ikot, G. J. Rampho, R. Sever, Commun. Theor. Phys, 71, 1246-1252, (2019).

[81] C. Beck, Brazilian Journal of Physics, vol. 39, No. 2A, 357-362, (2009).

[82] A. Kyniene, G. Merkelis, A. Sukys, S. Masys, S. Pakalka, R. Kisielius, V. Jonauskas, J. Phys. B: At. Mol. Opt. Phys. 51, 155202, 7pp, (2018).

[83] M. Goto, T. Fujimmoto, NIFS-DATA-43, (1997).

[84] S. B. Hansen, PHYSICAL REVIEW E 70, 036402, (2004).

Chapter 3

Calculation of ionization rates from superstatistics

3.1 Introduction

The properties of non-equilibrium plasmas is determined through the ionization of atoms and molecules by electron impact (EII), which is of great practical importance including low- and high-temperature laboratory plasmas [1]. Therefore, in collisional plasma, the ionization state is limited by ionization rates, EII can also have a significant effect on the charge state distribution for plasmas with a non-thermal electron energy distribution [2].

On the other hand, ionization occurs when an electron collides with a neutral particle with enough energy to produce a positive ion and also a free electron [3]. Moreover, the value of a precise assessment of ionization cross sections is demonstrated by the broad range of physical phenomena whose meanings necessitate the knowledge of ionization by electron impact reaction rates [4, 5], This allows the determination of reasonably accurate cross-section functions which are required for the application branches[6].

It is necessary to have knowledge of these rates. Consequently, we depend on the Maxwellian, non-Maxwellian distributions, and the Beck-Cohen superstatistics. Additionally, we shall show the influence of superstatistics on non-thermal and superthermal distributions on the calculation of ionization rates for Helium, Beryllium, and Lithium like Helium by the concept of superstatistics.

During our work, we take a different new idea that consists in replacing the distribution function through the effective Boltzmann factor to using superstatistics and introducing the formalism of superstatistics in the case of ionization rates in various ways. Such an approach has a great advantage: More

general statistics can be generated following different forms of fluctuations.

The outline of this chapter is as follows, firstly we present the calculation of ionization rates using the formalism of superstatistics with various values of q. Then, we introduce the influence of electron energy distribution functions on the calculation of ionization rates for neutral Helium (He) and particularly establish the effects of hot electrons fraction with different values.

Secondly, we show the influence of superstatistics on nonthermal and suprathermal distributions on the calculation of ionization rates for Beryllium, and Lithium ions (Be^{+2}, Li^{+}), where we replace the distribution function with an effective Boltzmann factor. Thirdly, we report and discuss the results and we make comparisons with previous studies that present the influence of electron energy distribution functions on the calculation of ionization rates.

3.2 Calculation of ionization rates

In 2003, new statistics is shown by Beck and Cohen which is known as superstatistics concept. Superstatistics is a combination of two (or more) various statistics: one based on Boltzmann factors and the other on large-scale fluctuations of one (or more) demanding parameters (e.g. the inverse temperature) [7]. They usually work with non-equilibrium conditions that have a long-term stationary case and a spatiotemporally fluctuating intense quantity [8].

The study of non-linear and nonequilibrium systems is the focus of superstatistics, a branch of statistical mechanics or statistical physics. To accomplish the desired non-linearity, it employs the superposition of numerous independent statistical models [9]. The framework of this theory assumes that the correct ensemble is not canonical, but a superposition of canonical ensembles at different β weighted by a factor $f(\beta)$ [10]. Also, this formalism can only be applied if the system has enough time to find local equilibrium in the local small cells with a given β. In these cells, local equilibrium statistical mechanics is valid. Hence, for the whole system, instead of the standard Boltzmann factor, Beck [8] introduces another quantity written as follows:

$$B(E) = \int_0^\infty f(\beta) e^{-\beta E} d\beta \tag{3.1}$$

The $B(E)$ function is the generalized Boltzmann factor for the non-equilibrium system, $f(\beta)$ is the distribution function, $e^{-\beta E}$ is the Boltzmann factor and E

is the energy level for the system. So, the superstatistics, denoted by symbol $B(E)$, allows the infinite types of system's distribution with respect to E, once the fluctuating distribution $f(\beta)$ is given [11].

With regards to the question about evaluating the generalized Boltzmann function $B(E)$, it is noted, in the literature, that there are two approximations: low-E and high-E asymptotics. The low energy asymptotics of superstatistics was previously discussed by Beck [9].

He exhibits that while in general, the large E behavior is different for all superstatistics (it strongly depends on the function $f(\beta)$), the low E (low-energy asymptotics) behavior is universal for all superstatistics. Beck shows that this approximation represents the leading order correction to ordinary statistical mechanics for the nonhomogeneous system with temperature fluctuations of small values of the energy E behavior can be shown universally. Following this approximation, Beck proved, for any distribution $f(\beta)$, that the generalized Boltzmann factor $B(E)$ is written as [9, 12]:

$$
\begin{aligned}
B(E) &= \langle e^{-\beta E} \rangle && (3.2)\\
&= e^{-\beta_0 E} e^{+\beta_0 E} \langle e^{-\beta E} \rangle && (3.3)\\
&= e^{-\beta_0 E} \langle e^{-(\beta-\beta_0)E} \rangle && (3.4)\\
&= e^{-\beta_0 E} \left(1 + \frac{1}{2}\sigma^2 E^2 + \sum_{r=3}^{\infty} \frac{(1)^r}{r!} \langle (\beta - \beta_0)^r \rangle E^r \right) && (3.5)
\end{aligned}
$$

The r is the moments of the distribution $f(\beta)$ about the mean, which are the coefficients of the powers E_r in this case, can be written in terms of the ordinary moments as:

$$
\langle (\beta - \beta_0)^r \rangle = \sum_{j=0}^{r} \binom{r}{j} \langle \beta^j \rangle (-\beta_0)^{r-j} \tag{3.6}
$$

With $\langle \beta \rangle = \beta_0 = \int_0^\infty \beta f(\beta) d\beta$ and $\sigma^2 = \langle \beta^2 \rangle - \langle \beta \rangle^2$ are the average and the variance respectively. The zeroth-order approximation to $B(E)$ corresponds, as is expected, to the "pure" Boltzmann statistics:

$$
B(E_n) \sim e^{-(\beta) E_n}
$$

This universality showed that the superstatistics theory is controlled by two universal parameters (β, q) with:

$$q = \frac{\langle \beta^2 \rangle}{\langle \beta \rangle^2} \tag{3.7}$$

In the (Eq.(3.7)), the parameter q is just the coefficient of variation of the distribution $f(\beta)$, defined by the ratio of standard deviation and mean. This parameter controls the fluctuation of the intensive parameter β. If there are no fluctuations at all, we obtain $q = 1$ as required [7].

3.3 Ionization rates of neutral Helium

3.3.1 Simulation methodology

Whether for experimental or cosmical plasmas, ionization rates for various ions are important in knowing the ionization phenomenon. The process of ionization from metastable states is also important in the experiment, for electron impact effects at some temperature T_e is given by averaging the energy-dependent cross-section σ for the distribution of electron velocity v. The ionization rate τ may be given as a cross-section's function of ionization by the next integral [13]:

$$\tau = \int v\sigma(E) f(E) dE \tag{3.8}$$

Where $v = \sqrt{\frac{2E}{m}}$, and m are the velocity and mass of electron, and $f(E)$ is the electron energy distributions function.

In previous studies, researchers used two types of Maxwellian or non-Maxwellian distribution functions in the ionization rates. Indeed superstatistics presents an effective description of their tools since they have shown their flexibility in advanced research. Therefore, in our work, to calculate the ionization rates from cross-sections in our work FAC code of neutral Helium, we replace $f(E)$ with effective Boltzmann factor $B(\beta)$ to using Superstatistics and non-Maxwellian distribution function.

As result, the ionization rates become:

$$\tau = \int v\sigma(E) f_{NM}(E) dE \tag{3.9}$$

We have

$$B(E) = e_q^{-\beta_0 E}$$

The distribution function in a particular system describes the density distribution of particles around a reference particle as a basis of influential parameters of a system. The common distribution functions are two; Maxwellian and non-Maxwellian. One of the basic principles of physics, exploited in the physics of the solar corona, is the Maxwellian distribution of electrons and ions. Distribution functions $f(E)$ are given by the concept of temperature are only valid for a Maxwellian distribution, which is written as (with $E = \frac{1}{2}mv^2$, where E is the energy and m the mass of the electron) [13]:

$$f_M(E) = \frac{2}{\sqrt{\pi}}\left(\frac{1}{T}\right)^{\frac{3}{2}} \sqrt{E} e^{-\frac{E}{T}} \tag{3.10}$$

Where T is temperature.

When the hot electrons are interesting in plasma, in order to detect the main mechanisms, the non-Maxwellian function is given by:

$$f_{NM}(E) = (1 - f_{hot}) f_M(T_{bulk}) + f_{hot} f_M(T_{hot}) \tag{3.11}$$

f_M the Maxwell energy distribution function, f_{hot} is the normalized hot electron fraction, and T_{hot} and T_{bulk} are, respectively, the hot and bulk electron temperature [13].

We depend in our work on the non-Maxwellian function to calculate the ionization rates of Helium ions. This function has an exact role in the behavior of electrons in the plasma Helium that is related to the temperature.

Therefore

$$\tau = \int v\sigma(E)[(1 - f_{hot}) f_M e_q^{-\beta_0 E}(T_{bulk}) + f_{hot} f_M e_q^{-\beta_0 E}(T_{hot})]dE \tag{3.12}$$

Now, according to the following works of Tsallis, the non-extensive statistics of Tsallis defined by the so-called q-exponential function

$$e_q^{-\beta_0 E} = (1 + (q-1)\beta_0 E)^{-\frac{1}{q-1}} \tag{3.13}$$

With the q-exponential function is defined by:

$$e_q(x) = \begin{cases} (1+(q-1)\beta_0 E)^{-\frac{1}{q-1}} & 0 < q < 1 \\ e^x & q = 1 \end{cases}$$

Where the parameter q is the index of non-extensive statistical mechanics.

3.3.2 Results and discussion

The ionization rates of neutral Helium are generated from cross sections obtained by the Flexible Atomic Code (FAC), weighted by a non–Maxwellian distribution function. The results are compared to those reported by Kato et al. [14]. In these calculations, we rely on Python programming (Spyder Python 3.9.7) by writing a special code (A).

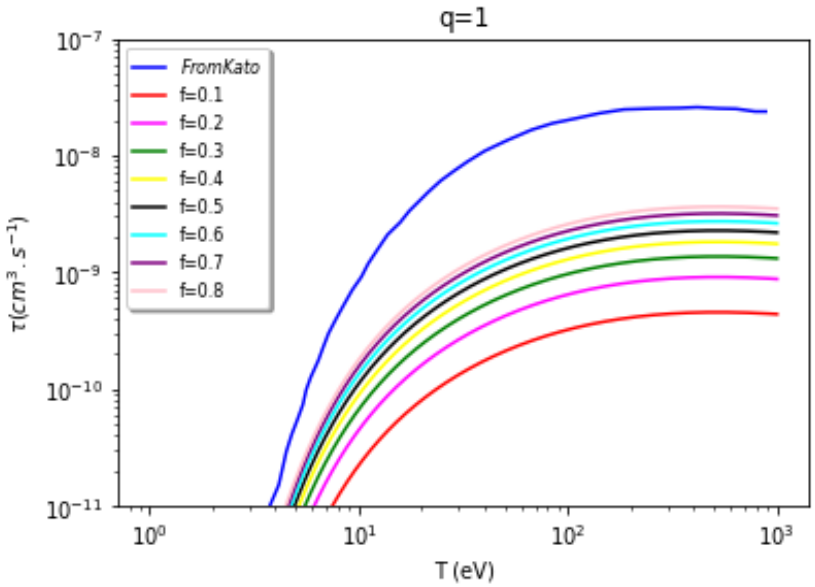

Figure 3.1: The ionization rates of He: The coefficients rates are obtained using a non–Maxwellian distribution function with $q = 1$ and the effects of various hot electrons fraction f_{hot}.

Fig.3.1 presents the results of calculating the ionization rates of neutral helium, where $q = 1$. The curves have maxima at approximately 100 eV for all states, and the ionization rates calculated amount to more than $10^{-9} cm^3 s^{-1}$ when the value of hot electrons fraction $f_{hot} = 0.8$.

Fig.3.1 shows a high level of agreement between the designed curves for various values of hot electrons fraction f_{hot}. We also show that the curves become closer to each other until they virtually cling together as the hot electrons

fraction increases because superstatistics and the well-known maxwell statistic have certain similarities when $q = 1$.

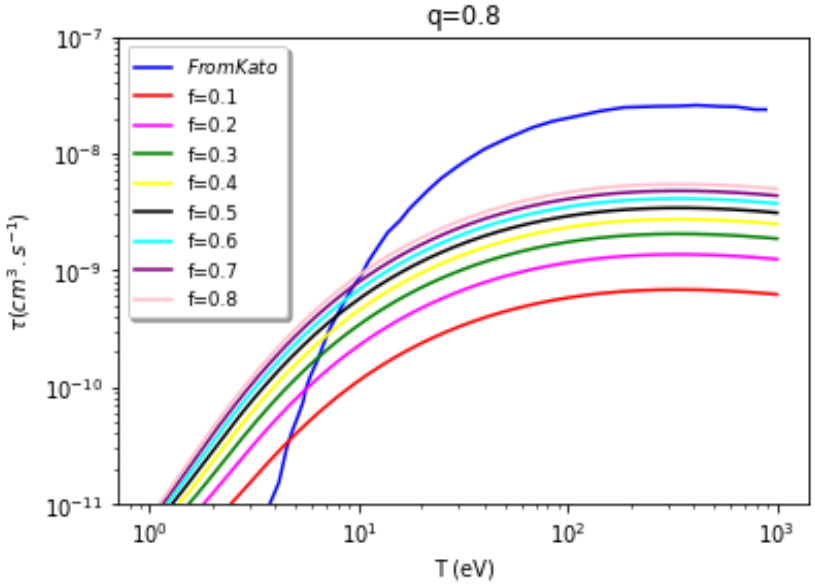

Figure 3.2: The ionization rates of He: The coefficients rates are obtained using a non–Maxwellian distibution function with $q = 0.8$ and the effects of various hot electrons fraction f_{hot}.

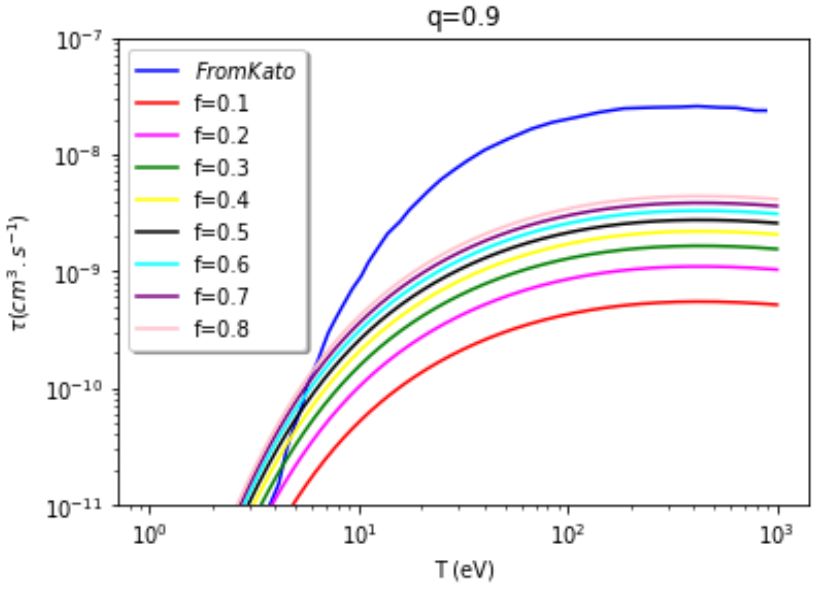

Figure 3.3: The ionization rates of He: The coefficients rates are obtained using a non–Maxwellian distribution function with $q = 0.9$ and the effects of various hot electrons fraction f_{hot}.

Fig.3.2 and Fig.3.3 present the ionization rates of He obtained by superstatistics where: $q = 0.8$ and $q = 0.9$. They show how superstatistics change the ionization rates of neutral helium as a result of variations in the hot electrons

fraction.

The ionization rates begin to deviate at the value 10 eV in the case of $q = 0.9$, and the experiment curve[14]intersects with all the curves of ionization rates except in the case of $f_{hot} = 0.1$; this implies that the superstatistics coincides with the experiment results[14].

On the other hand, in the case of $q = 0.8$, the curves deviate at energy ($1eV$), while the experiment curve intersects with all the ionization rates curves. In addition to that, a convergence focus between the rates as the fraction of the hot electron f_{hot} increases. Moreover, it shows some congruence between the three values highest exactly at $f_{hot} = 0.6, 0.7, 0.8$.

These curves show the inverse relation of ionization rates with the behavior of the generalized Boltzmann distribution, which are presented by (K. OURABAH et.al) in Fig.3.1 [15].

In addition, we note that the ionization rates increase with high energy so as the intensity of ionization by electron impact until it reaches the stage of full ionized plasma, and hence the curves become stable.

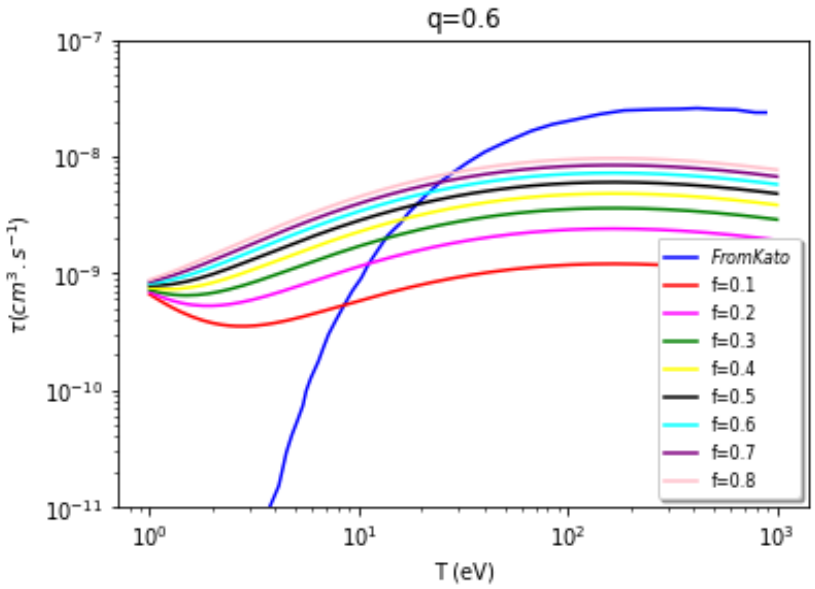

Figure 3.4: The ionization rates of He: The coefficients rates are obtained using a non–Maxwellian distribution function with $q = 0.6$ and the effects of various hot electrons fraction f_{hot}.

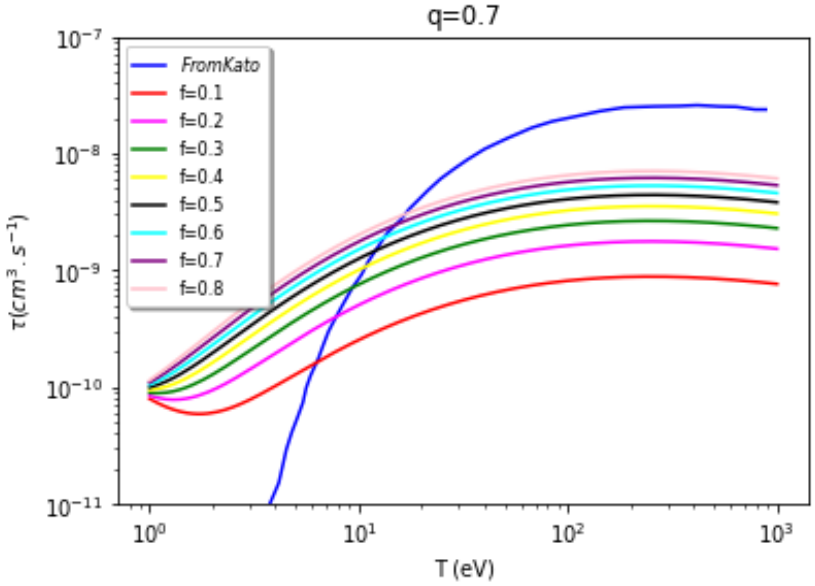

Figure 3.5: The ionization rates of He: The coefficients rates are obtained using a non–Maxwellian distribution function with $q = 0.7$ and the effects of various hot electrons fraction f_{hot}.

Fig.3.4 and Fig.3.5 present the ionization rates of He obtained by superstatistics where $q = 0.6$ and $q = 0.7$. In Figures 5 and 6, in the case where q has a low value, the curves of ionization rates deviate significantly throughout the energy range. We can note that there is a severe deviation for the value $q = 0.6$.

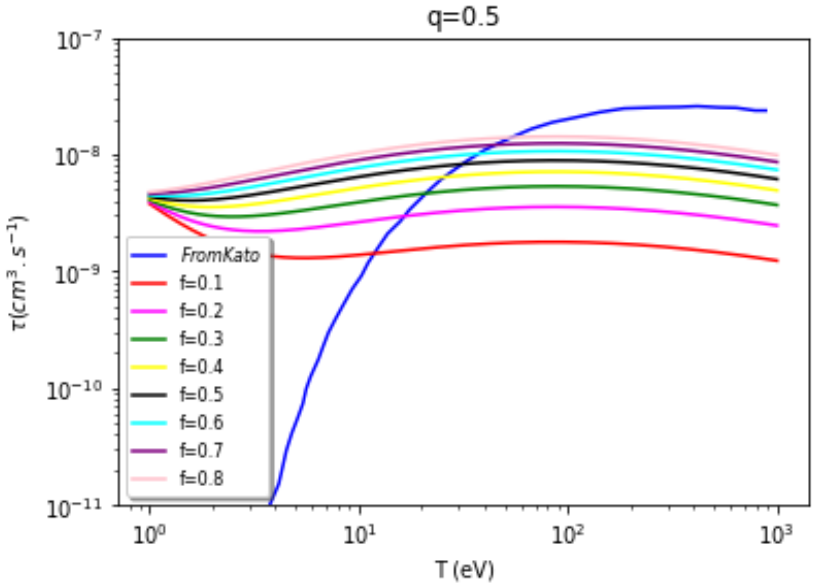

Figure 3.6: The ionization rates of He: The coefficients rates are obtained using a non–Maxwellian distribution function with $q = 0.5$ and the effects of various hot electrons fraction f_{hot}.

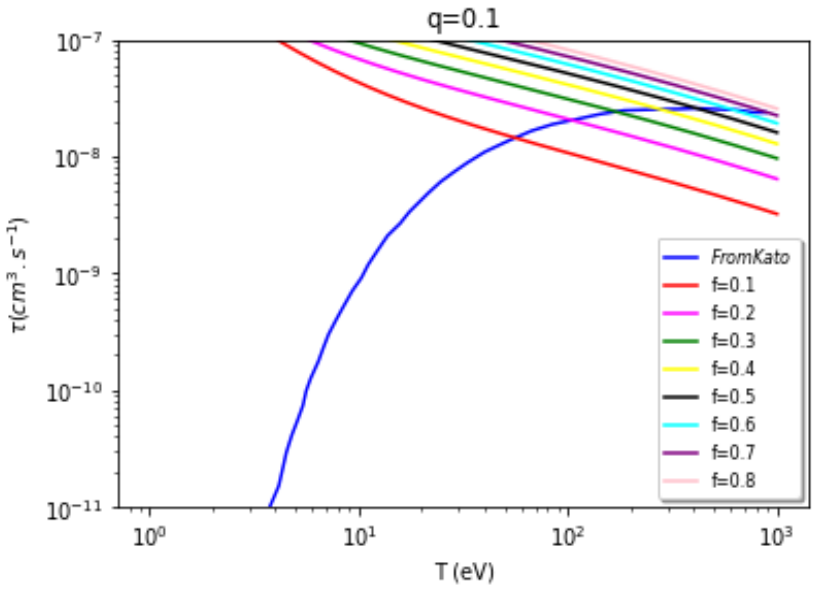

Figure 3.7: The ionization rates of He: The coefficients rates are obtained using a non–Maxwellian distribution function with $q = 0.1$ and the effects of various hot electrons fraction f_{hot}.

Fig.3.6 and Fig.3.7 present the ionization rates of He obtained by superstatistics where $q = 0.5$ and $q = 0.1$. The curves of Fig.3.6 and Fig.3.7, in case $q = 0.5$, confirm that the computed superstatistics ionization rates are significantly affected by the values of q and not by the non-Maxwellian distribution function. Intensities of the deviations increase as the value of $q = 0.1$ is decreased. Such an approach is expected to be a suitable approximation for a varying q field nearby ($q \in]0.7, 1]$).

It is interesting to mention that this interpretation provides somehow a unification of these different distributions encountered in plasma physics. It is well-known that temperature fluctuations occur often in plasma environments, and they contribute considerably to the particle flux [16] and drive a significant amount of the anomalously high electron heat transport [17]. Many observations indicate the existence of temperature fluctuations in astrophysical plasmas environments [18, 19] and in laboratory plasma devices.

Then, it appears very plausible to relate the anomalous distributions observed in plasmas to typical temperature fluctuations. We stress that a comparison of the experimental data of the temperature fluctuations is a problem of great importance. In deviated cases, however, we can explain this abnormal state to depend on Beck and Tsallis superstatistic, which displays that a superstatistical non-equilibrium system can be projected onto an ordinary statistical

mechanics equilibrium system with an inverse temperature [13, 20].

From the focus of these results, the theory of superstatistics forces the presence of temporally local equilibrium within the plasma Helium that appears as a non-equilibrium thermodynamic system. Thus, the introduction of the formalism of superstatistics in the case of ionization rates with various values of q, is limited to an agreement with the Kato et al. study of other statistics.

3.4 Ionization rates of Beryllium, and Lithium like Helium

3.4.1 Simulation methodology

Therefore, in this part, to calculate the ionization rates from cross-sections of Beryllium, Lithium ions (Be^{+2}, Li^{+}), we replace $f(E)$ with effective Boltzmann factor $B(E)$ to using superstatistics [21].

When we use the effective Boltzmann factor.

$$B(E) = e^{-\beta_0 E}\left(1 + \frac{1}{2}(q-1)\beta_0^2 E^2 + g(q)\beta_0^3 E^3 ....\right) \tag{3.14}$$

Where the factor $g(q)$ refers to:

$$g(q) = 0 \qquad \text{(uniform and 2-level)} \tag{3.15}$$

$$= -\frac{1}{3}(q-1)^2 \qquad \text{(Gamma)} \tag{3.16}$$

$$= -\frac{1}{6}(q^3 - 3q + 2)^2 \qquad \text{(log-normal)} \tag{3.17}$$

$$= -\frac{1}{3}\frac{(q-1)(5q-6)}{3-q} \qquad \text{(F-distribution with v = 4)} \tag{3.18}$$

So, to calculate the ionization rates from cross-sections, we replace $f(E)$ to effective Boltzmann factor $B(E)$ to using superstatistics.

$$\tau = \int v\sigma(E) e^{-\beta_0 E}\left(1 + \frac{1}{2}(q-1)\beta_0^2 E^2 + g(q)\beta_0^3 E^3 ....\right) dE \tag{3.19}$$

3.4.2 Results and discussion

◇ Ionization rates of Beryllium ions (Be^{+2})

In these calculations, we rely on Python programming (Spyder Python 3.9.7) by writing a special code (B).

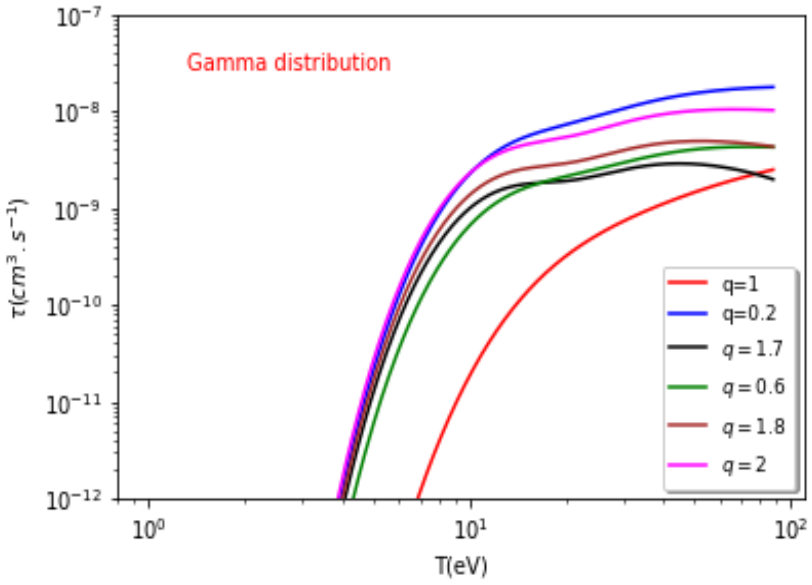

Figure 3.8: Coefficients of the ionization rates of Be^{+2}: obtained using various values from q by Gamma distribution.

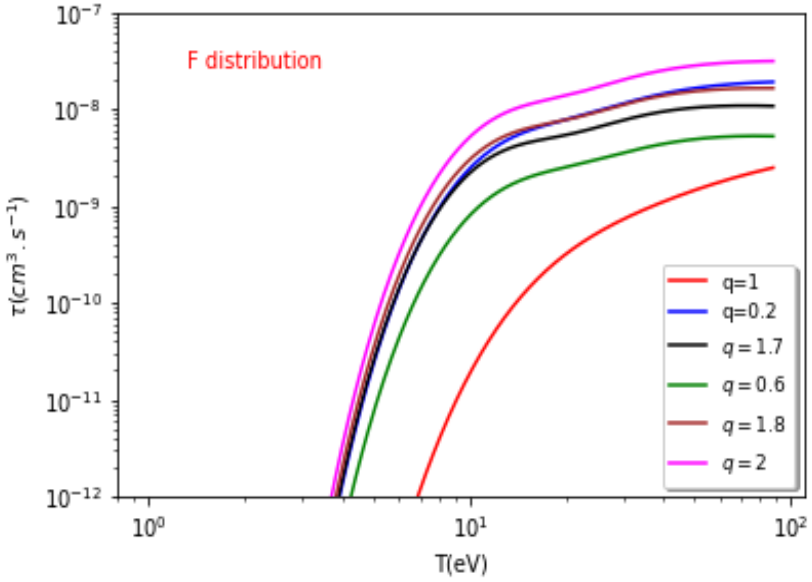

Figure 3.9: Coefficients of the ionization rates of Be^{+2}: obtained using various values from q by F-distribution.

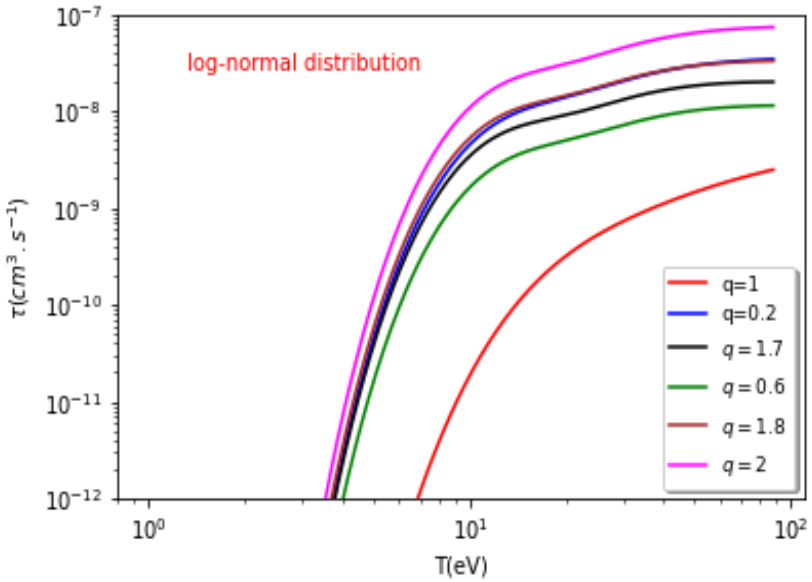

Figure 3.10: The ionization rates for Be^{+2}: obtained using various values for q by Log-normal distribution.

The coefficient rates are obtained using the various $g(q)$ functions, where they rely on the superstatistics concept. It is important to use the superstatistics approach in the calculation of the ionization rates for Be^{+2}. The ionization rates decrease when the value q increases. Where the greatest one is at $q = 1$. Also, it's seemed that there is a rapprochement between the curves at the same distribution. We can note that it is nice coordination between the curves and for the three functions and in particular for the low values of q.

◇ Ionization rates of Lithium ions (Li^{+})

In these calculations, we rely on Python programming (Spyder Python 3.9.7) by writing a special code (B).

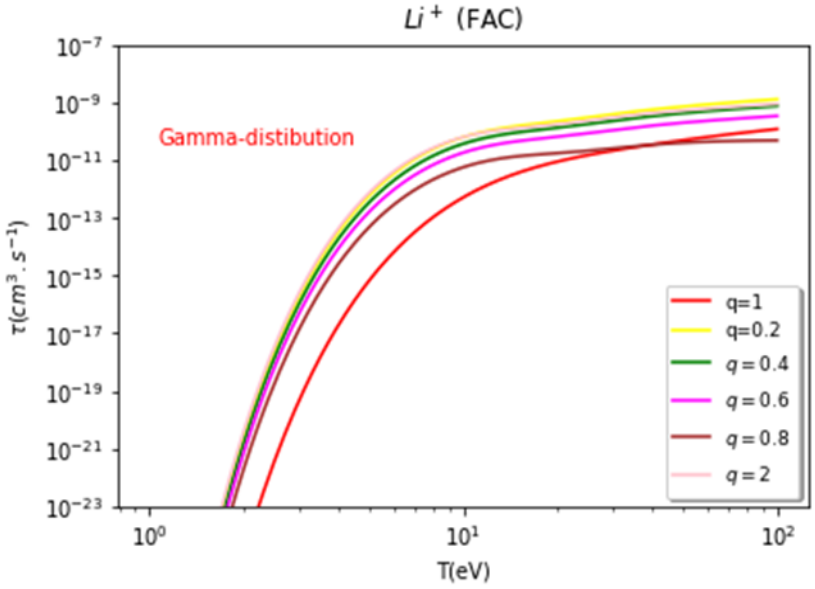

Figure 3.11: Coefficients of the ionization rates of Li on: obtained using of various values from q by Gamma distribution.

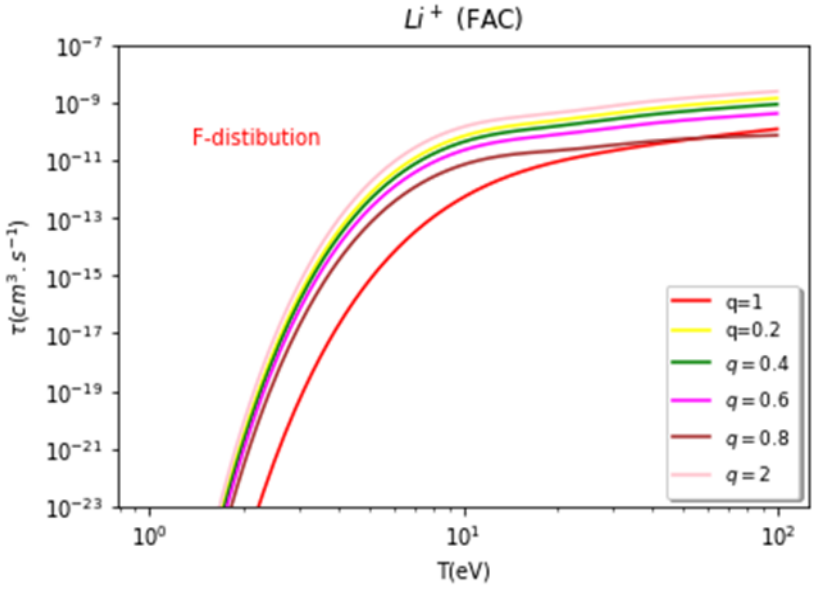

Figure 3.12: Coefficients of the ionization rates of Li ion: obtained using of various values from q by F-distribution.

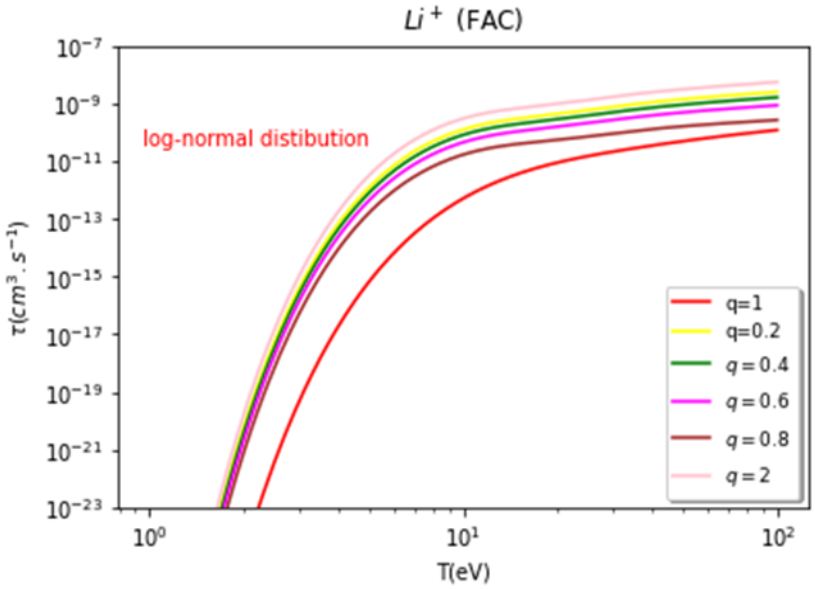

Figure 3.13: Coefficients of the ionization rates of Li ion: obtained using of various values from q by log-normal distribution.

The rates of coefficients are obtained using the various $g(q)$ functions, where they rely on the superstatistics concept. It is important to note that through using the superstatistics approach in the calculation of the ionization rates for Li ions (Li^-), there is nice coordination between the curves and that for the three functions and in particular for the low values of q.

3.5 Conclusion

In our work, we aimed to deal with the physical explanation of the two famous empirical distributions, namely, the suprathermal and the nonthermal ones. A connection between these non-Maxwellian distributions and superstatistics is suggested. Using the Beck–Cohen superstatistics, we interpret these two distributions as a consequence of temperature fluctuations. It is interesting to mention that this interpretation provides somehow a unification of these different distributions encountered in plasma physics.

Ionization rates of neutral Helium are calculated using cross sections computed using the Flexible Atomic Code (FAC), with the distribution function replaced with an effective Boltzmann factor, superstatistics, and a non-Maxwellian distribution function. The results show a good agreement between the designed curves for various values of hot electrons fraction f_{hot} because superstatistics and the statistic Maxwellian have similarities when q is close to 1.

However, in the case of deviations, they are applied to a superstatistical non-equilibrium system, which has been done onto an ordinary statistical mechanics equilibrium system with an inverse temperature. Furthermore, the theory of superstatistics forces the presence of temporally local equilibrium within the plasma Helium that appears a non-equilibrium thermodynamic system. Thus, the introduction of the formalism of superstatistics in the case of ionization rates with various values of q, is limited to an agreement with Kato et al. and other statistics.

Additionally, The ionization rates of Be^{+2} are calculated using cross sections computed using the Flexible Atomic Code (FAC), with the distribution function replaced with an effective Boltzmann factor and different forms of distribution functions. The results show good agreement between the designed curves for various values of q because superstatistics and the statistic Maxwellian have similarities when q is close to 1. However, the deviations are applied to a superstatistical non-equilibrium system that has been done onto an ordinary statistical mechanics equilibrium system with an inverse temperature.

Besides, the theory of superstatistics forces the presence of temporally local equilibrium within the plasma helium that appears as a non-equilibrium thermodynamic system. Thus, the introduction of the formalism of superstatistics in the case of ionization rates with various values of q, which is limited to an agreement with other statistics. We can see the connection between the Maxwellian distributions and the Beck-Cohen superstatistics, where we have shown the relation between the superstatistics approach as well as the low values of q less than 1 on the calculation of ionization rates of Beryllium ions (Be^{+2}).

Finally, We can see the connection between the Maxwellian distributions and the Beck-Cohen superstatistics, where we have shown the relation between the superstatistics approach as well as the low values of q less than 1 on the calculation of ionization rates of Lithium like Helium.

References

[1] L. J. Kieffkr, G. H. Dunn, Rev. Mod. Phys. 38 (1), (1966).

[2] S. Davis, J. Jain, D. Gonzalez, G. Gutierrez, IOP Conf. Series: Journal of Physics: Conf. 1043, 012011, (2018).

[3] A. Chachereau, S. Pancheshnyi, IEEE Trans. Plasma Sci. 42 (10) (2014).

[4] M. R. H. Rvdge, Rev. Modern Phys. 40 (3), (1968).

[5] A. F. Tseluyko, V. T. Lazurik, D. L. Ryabchikov, V. I. Maslov, N. A. Azarenkov, I. N. Sereda, D. V. Zinovev, N. N. Yunakov, A. A. Makienko, Probl. At. Sci. Technol. 1, 165–167, (2009).

[6] D. Margreiter, H. Deutsch, T. D. Mgrk, Int. J. Mass Spectrom. Ion Process. 139, 127–139, (1994).

[7] C. Beck, Physica A 342, 139 – 144, (2004).

[8] C. Beck, Physica A 365, 96–101, (2006).

[9] C. Beck, E. G. D. Cohen, Physica A 322, 267 – 275, (2003).

[10] C. Beck, Phil. Trans. R. Soc. A, 369, 453–465, (2011).

[11] T. Yamano, Progr. Theoret. Phys. 162, 87–96, (2006).

[12] F. Khalfaoui, S. Dilmi, A. Boumali, Physica A, 596, 127193, (2022).

[13] S. B. Hansen, A.S. Shlyaptseva, Phys. Rev. E 70, 036402, (2004).

[14] T. Kato, K. Masai, M. Arnaud, NIFS-Data-Series 14, (1991).

[15] H. Touchette, C. Beck, Phys. Rev. E 71, 016131, (2005).

[16] R. Kumar, S. K. Saha, Pramana 55,713, (2000).

[17] H. J. Hartfuss, S. Sattler, M. Hase, M. Hirsch, T. Geist, W7-AS Team, Fusion Eng. Des. 34,81, (1997).

[18] C. Esteban, Astrophys. Space Sci. 263,193 (1998).

[19] A. F. Kholtygin, V. F. Bratsev, V. I. Ochkur, Astrophysics 45,32, (2002).

[20] C. Tsallis, A. M. C. Souza, Phys. Rev. E 67, 026106, (2003).

[21] K. P. Dere, A&A 466, 771–792, (2007).

General conclusion

Through our project, we calculated ionization rates by the formalism of superstatistics. Where we introduced the influence of electron energy distribution functions on the calculation of ionization rates for neutral Helium. Also, we showed the effects of hot electron fraction on it. Besides, we presented the influence of superstatistics on nonthermal, and suprathermal distributions of the ionization rates for Beryllium, and Lithium ions (Be^{+2}, Li^{+}).

In order to do that, we replaced the distribution function with an effective Boltzmann factor which was suggested by Beck and Cohen in 2003. After that, we discussed the results and presented comparisons with other studies, that present the influence of electron energy distribution functions on the calculation of ionization rates.

Firstly, we started with generalities on plasmas to present their importance in scientific research because they are widely used in wide technology domains. On the other hand, we showed the various equilibrium models. Moreover, we did a comparison of elementary processes in hot plasmas, which contain such as ionization as the main process, excitation, radiative transition, photoionization, and recombination.

Secondly, we focused on electron impact ionization which leads to creating plasmas. Furthermore, we exhibited the different kinds to calculate cross sections, both the empirical and semi-empirical or the calculation codes. Then we showed the distribution functions (Maxwell, non-Maxwellian, Gaussian, Power Law, etc).

We also discussed superstatistics distribution, which is superpositions of two (or more) unlike other statistics: one is given by ordinary Boltzmann factors, and the other by large-scale fluctuations of one (or many) intensive parameters(e.g. the inverse temperature), Since then, it has served as a useful method

for describing a wide range of dynamic structures with changing environmental conditions. Finally, the ionization rate coefficient is presented as the basis of our work.

In the experimental part, we aimed to deal with the physical explanation of the two famous empirical distributions, namely, the suprathermal and the non-thermal ones. A connection between these non-Maxwellian distributions and superstatistics is suggested. Using the Beck–Cohen superstatistics, we interpret these two distributions as a consequence of temperature fluctuations. It is interesting to mention that this interpretation provides somehow a unification of these different distributions encountered in plasma physics.

Ionization rates of neutral Helium are calculated using cross sections computed using the Flexible Atomic Code (FAC), with the distribution function replaced with an effective Boltzmann factor, superstatistics, and a non-Maxwellian distribution function. The results show a good agreement between the designed curves for various values of hot electrons fraction f_{hot} because superstatistics and the statistic Maxwellian have similarities when q is close to 1.

However, in the case of deviations, they are applied to a superstatistical non-equilibrium system, which has been done onto an ordinary statistical mechanics equilibrium system with an inverse temperature. Furthermore, the theory of superstatistics forces the presence of temporally local equilibrium within the plasma Helium that appears a non-equilibrium thermodynamic system. Thus, the introduction of the formalism of superstatistics in the case of ionization rates with various values of q, is limited to an agreement with Kato et al. and other statistics.

Additionally, The ionization rates of Be^{+2} are calculated using cross sections computed using the Flexible Atomic Code (FAC), with the distribution function replaced with an effective Boltzmann factor and different forms of distribution functions. The results show good agreement between the designed curves for various values of q because superstatistics and the statistic Maxwellian have similarities when q is close to 1. However, the deviations are applied to a superstatistical non-equilibrium system that has been done onto an ordinary statistical mechanics equilibrium system with an inverse temperature.

Besides, the theory of superstatistics forces the presence of temporally local equilibrium within the plasma helium that appears as a non-equilibrium thermodynamic system. Thus, the introduction of the formalism of superstatistics in the case of ionization rates with various values of q, which is limited to an agreement with other statistics. We can see the connection between the Maxwellian distributions and the Beck-Cohen superstatistics, where we have shown the relation between the superstatistics approach as well as the low values of q less than 1 on the calculation of ionization rates of Beryllium ions (Be^{+2}).

Finally, We can see the connection between the Maxwellian distributions and the Beck-Cohen superstatistics, where we have shown the relation between the superstatistics approach as well as the low values of q less than 1 on the calculation of ionization rates of Lithium.

Chapter A

Appendix 1

◇ Method for calculating ionization rates for neutral Helium from Python

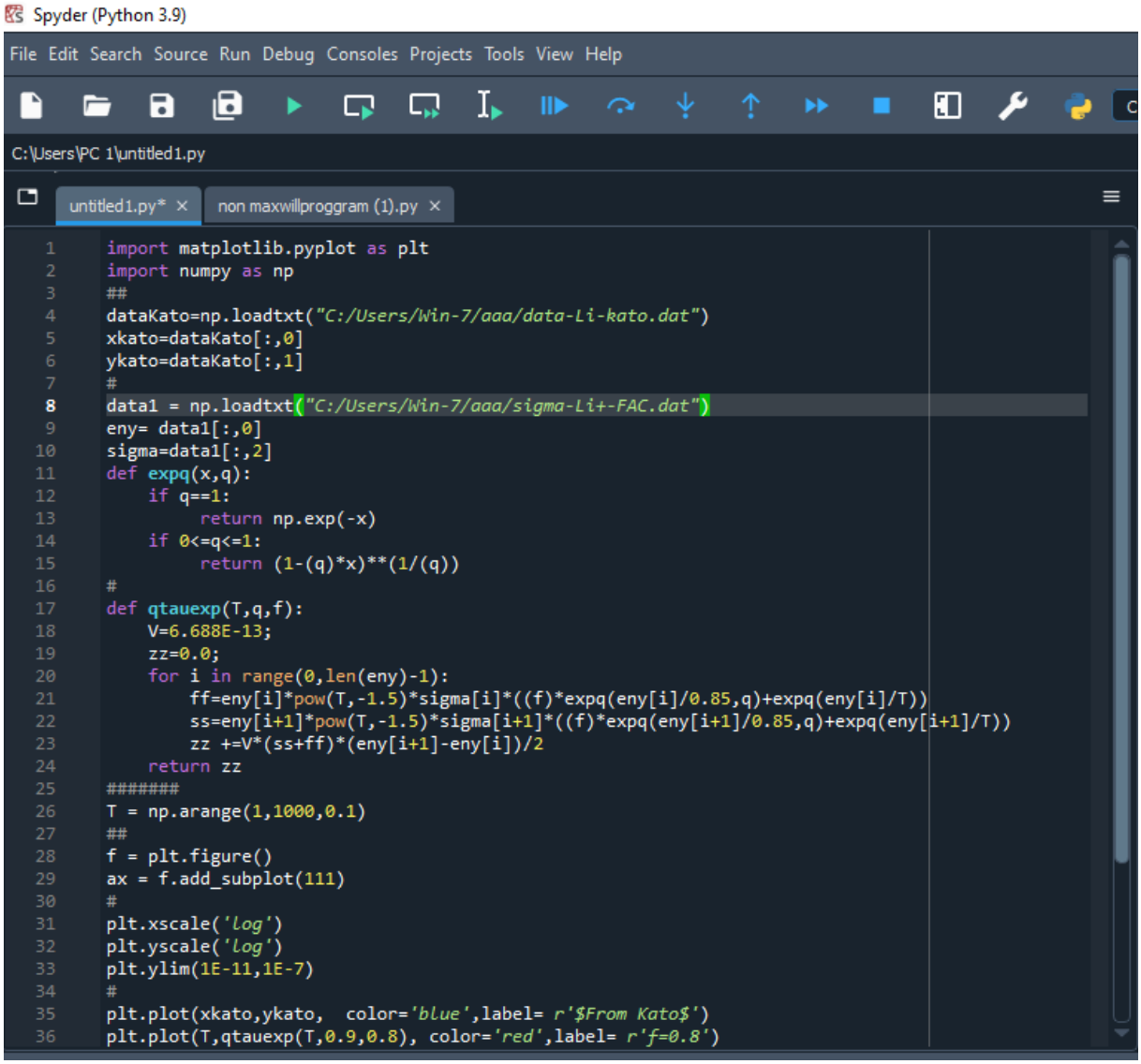

```
35  plt.plot(xkato,ykato,  color='blue',label= r'$From Kato$')
36  plt.plot(T,qtauexp(T,0.9,0.8), color='red',label= r'f=0.8')
37  plt.plot(T,qtauexp(T,0.9,0.1),  color='magenta',label= r'f=0.1')
38  plt.plot(T,qtauexp(T,0.9,0.3),  color='green',label= r'f=0.3')
39  plt.plot(T,qtauexp(T,0.9,0.5), color='yellow',label= r'f=0.5')
40  plt.plot(T,qtauexp(T,0.9,0.7), color='black',label= r'f=0.7')
41  ax.set_title('Li-FAC: q=0.9')
42  plt.legend(shadow=True, fancybox=True,loc='lower right',prop={'size':9})
43
44
```

Chapter B

Appendix 2

◇ Method for calculating ionization rates for Li^{+} and Be^{+2} like Helium from Python

Spyder (Python 3.9)

File Edit Search Source Run Debug Consoles Projects Tools View Help

C:\Users\PC 1\.spyder-py3\temp.py

temp.py* × tauv.py ×

```
from math import sqrt,pi
import matplotlib.pyplot as plt
import pylab as pl
import numpy as np

dataKato=np.loadtxt("C:/Users/Win-7/aaa/data He-kato.txt")
xkato=dataKato[:,0]
ykato=dataKato[:,1]
#
data1 = np.loadtxt("C:/Users/Win-7/aaa/sigma-Li+-FAC.dat")
eny= data1[:,0]
sigma=data1[:,2]
V=6.688E-13
def tauG(T,n,q):
        zz=0.0
        for i in range(0,len(eny)-1):
         g= -(q-1)**2/3
##
         B1 = 1.0+0.5*(q-1)*(eny[i]**2)+g*(eny[i]**3/T**3)
         B2 = 1.0+0.5*(q-1)*(eny[i+1]**2)+g*(eny[i+1]**3/(T**3))
         ff=eny[i]*pow(T,1.5)*sigma[i]*np.exp(-eny[i]/T)
         ss=eny[i+1]*pow(T,1.5)*sigma[i+1]*np.exp(-eny[i+1]/T)
         zz +=V*(ss+ff)*(eny[i+1]-eny[i])/2
        return zz
############################
def taulogN(T,n,q):
       zz = 0.0
       for i in range(0,len(eny)-1):
        g= -(q**3-q+2)/6
        B1 = 1.0+0.5*(q-1)*(eny[i]**2)+g*(eny[i]**3/T**3)
        B2 = 1.0+0.5*(q-1)*(eny[i+1]**2)+g*(eny[i+1]**3/T**3)
        ff=eny[i]*pow(T,1.5)*sigma[i]*np.exp(-eny[i]/T)
        ss=eny[i+1]*pow(T,1.5)*sigma[i+1]*np.exp(-eny[i+1]/T)
        zz +=V*(ss+ff)*(eny[i+1]-eny[i])/2
        return zz
def tauF(T,n,q):
```

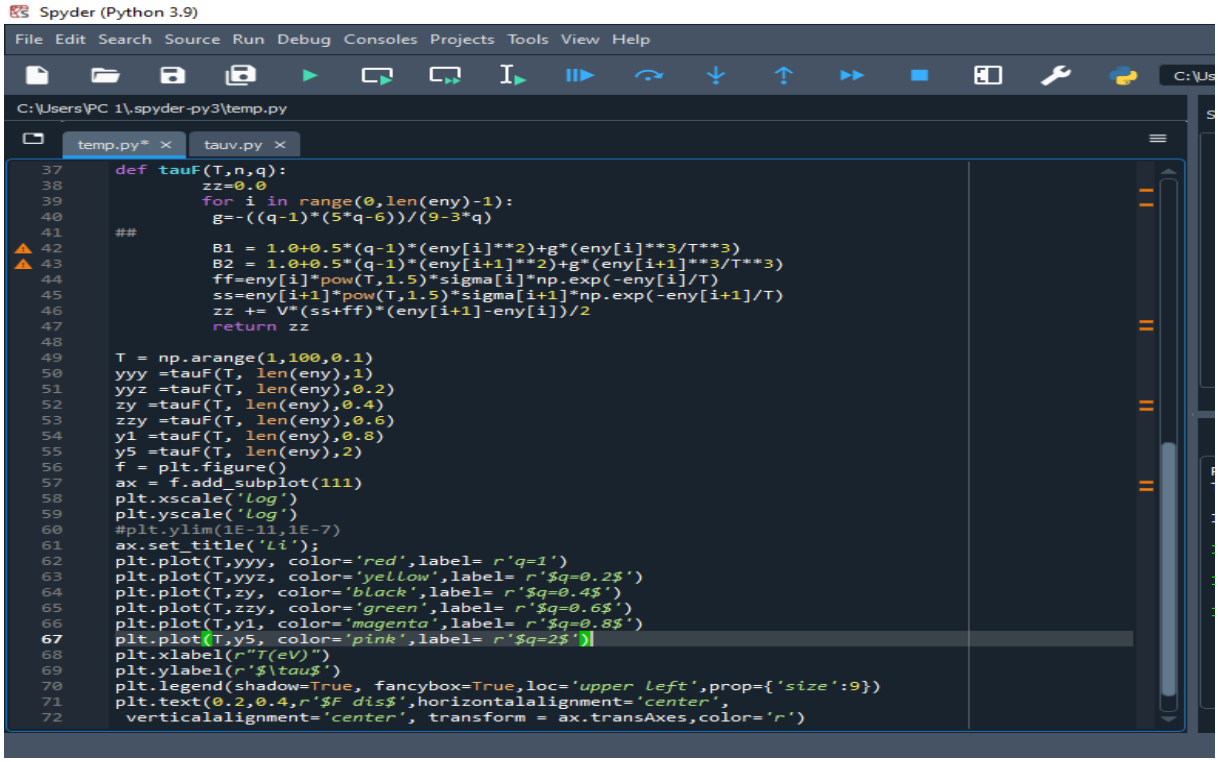
Spyder (Python 3.9)
File Edit Search Source Run Debug Consoles Projects Tools View Help
C:\Users\PC 1\.spyder-py3\temp.py
temp.py*
tauv.py
def tauF(T,n,q):
zz=0.0
for i in range(0,len(eny)-1):
g=-((q-1)*(5*q-6))/(9-3*q)
##
B1 = 1.0+0.5*(q-1)*(eny[i]**2)+g*(eny[i]**3/T**3)
B2 = 1.0+0.5*(q-1)*(eny[i+1]**2)+g*(eny[i+1]**3/T**3)
ff=eny[i]*pow(T,1.5)*sigma[i]*np.exp(-eny[i]/T)
ss=eny[i+1]*pow(T,1.5)*sigma[i+1]*np.exp(-eny[i+1]/T)
zz += V*(ss+ff)*(eny[i+1]-eny[i])/2
return zz
T = np.arange(1,100,0.1)
yyy =tauF(T, len(eny),1)
yyz =tauF(T, len(eny),0.2)
zy =tauF(T, len(eny),0.4)
zzy =tauF(T, len(eny),0.6)
y1 =tauF(T, len(eny),0.8)
y5 =tauF(T, len(eny),2)
f = plt.figure()
ax = f.add_subplot(111)
plt.xscale('log')
plt.yscale('log')
#plt.ylim(1E-11,1E-7)
ax.set_title('Li');
plt.plot(T,yyy, color='red',label= r'q=1')
plt.plot(T,yyz, color='yellow',label= r'$q=0.2$')
plt.plot(T,zy, color='black',label= r'$q=0.4$')
plt.plot(T,zzy, color='green',label= r'$q=0.6$')
plt.plot(T,y1, color='magenta',label= r'$q=0.8$')
plt.plot(T,y5, color='pink',label= r'$q=2$')
plt.xlabel(r"T(eV)")
plt.ylabel(r'τ')
plt.legend(shadow=True, fancybox=True,loc='upper left',prop={'size':9})
plt.text(0.2,0.4,r'$F dis$',horizontalalignment='center',
verticalalignment='center', transform = ax.transAxes,color='r')

- ***Abstract :***

Electron-impact ionization (EII) can be important in dynamic systems where atoms are suddenly exposed to higher electron temperatures. EII can also have a significant effect on the charge state distribution for plasmas with a non-thermal electron energy distribution. In this work, we present the effects of hot electrons on the calculation of ionization rates for neutral Helium using superstatistics. We also exchange the distribution function with the effective Boltzmann factor of superstatistics. The ionization rates of neutral Helium are obtained from cross sections obtained by FAC code, are weighted by a non-Maxwellian distribution function. The results are compared to those reported by Kato. et. al. We note that Non-Maxwellian energy distribution for different fractions of hot electrons showed the effects of these rates on the fractions of hot electrons and the forms of ionization rates. We also expose the effect of superstatistics on the calculation of ionization rates of Beryllium and Lithium ions when we replace the distribution function by Boltzmann effective factors. The results show a good agreement between the Maxwellian statistics and the superstatistics.

- ***Keywords :***

Ionization rates, Boltzmann factor, Superstatistic, FAC code, Hot electrons, Distribution functions.

- ***Résumé :***

L'ionisation par impact électronique (EII) peut être importante dans les systèmes dynamiques où les atomes sont soudainement exposés à des températures d'électrons plus élevées. EII peut également avoir un effet significatif sur la distribution de l'état de charge pour les plasmas avec une distribution d'énergie électronique non thermique. Dans ce travail, nous présentons les effets des électrons chauds sur le calcul des taux d'ionisation de l'Hélium neutre à l'aide de superstatistiques. Nous échangeons également la fonction de distribution avec le facteur de Boltzmann effectif des superstatistiques. Les taux d'ionisation de l'Hélium neutre sont obtenus à partir des sections efficaces obtenues par le code FAC, sont pondérés par une fonction de distribution Non- Maxwellienne. Les résultats sont comparés à ceux rapportés par Kato. et. al. Nous notons que la distribution d'énergie Non- Maxwellienne pour différentes fractions d'électrons chauds a montré les effets de ces taux sur les fractions d'électrons chauds et les formes des taux d'ionisation. Nous exposons également l'effet des superstatistiques sur le calcul des taux d'ionisation des ions heliumoides Béryllium et Lithium lorsque nous remplaçons la fonction de distribution par le facteur effectif de Boltzmann. Les résultats montrent un bon accord entre les statistiques Maxwelliennes et les superstatistiques.

- ***Mots clés :***

Taux d'ionisation, Facteur de Boltzmann, Superstatistique, Code FAC, Électrons chauds, Fonctions de distribution.

- **ملخص:**

يمكن أن يكون التأين بالتأثير الإلكتروني مهمًا في الأنظمة الديناميكية حيث تتعرض الذرات فجأة لدرجات حرارة عالية للإلكترون. يمكن أن يكون للتأين بالتأثير الإلكتروني أيضًا تأثير كبير على توزيع حالة الشحن للبلازما مع توزيع الطاقة الإلكترونية غير الحرارية. في هذا العمل ، نقدم تأثيرات الإلكترونات الساخنة على حساب معدلات التأين للهيليوم باستخدام الإحصائيات الفائقة. نستبدل أيضًا دالة التوزيع بمعامل بولتزمان الفعال للإحصاءات الفائقة. يتم الحصول على معدلات التأين للهيليوم من المقاطع الفعالة التي تم الحصول عليها بواسطة برنامج FAC ، ويتم ترجيحها بواسطة دالة توزيع غير ماكسويلي. تمت مقارنة النتائج مع النتائج المنشورة من طرف كاتو و زملائه. نلاحظ أن توزيع الطاقة غيرالماكسويلي للإلكترونات الساخنة أظهر تأثير هذه المعدلات على معدل الإلكترونات الساخنة وأشكال معدلات التأين. نعرض أيضًا تأثير الإحصائيات الفائقة على حساب معدلات لأيونات البريليوم والليثيوم الشبيهة بالهليوم عندما نستبدل دالة التوزيع بمعامل بولتزمان الفعال. تظهر النتائج توافقًا جيدًا بين إحصائيات ماكسويل والإحصاءات الفائقة.

- **الكلمات المفتاحية:**

معدلات التأين، معامل بولتزمان، الإحصائيات الفائقة، برنامج FAC، الإلكترونات الساخنة ، دوال التوزيع.